

FINDING THE CRITICAL EXPONENT  $\gamma$  FOR A BINARY FLUID MIXTURE  
USING THE SCATTERING OF LIGHT

by

Sarah Burleson

A senior thesis submitted to the faculty of

Ithaca College

in partial fulfillment of the requirements for the degree of

Bachelor of Science

Department of Physics

Ithaca College

April 2011

Copyright © 2011 Sarah Burleson

All Rights Reserved

ITHACA COLLEGE

DEPARTMENT APPROVAL

of a senior thesis submitted by

Sarah Burleson

This thesis has been reviewed by the senior thesis committee and the department chair and has been found to be satisfactory.

---

Date

---

Dr. Matthew C. Sullivan, Advisor

---

Date

---

Dr. Luke Keller, Senior Thesis Committee Member

---

Date

---

Dr. Jacob Hale, Senior Thesis Committee Member

---

Date

---

Dr. Beth Ellen Clark Joseph, Chair

## ABSTRACT

### FINDING THE CRITICAL EXPONENT $\gamma$ FOR A BINARY FLUID MIXTURE USING THE SCATTERING OF LIGHT

Sarah Burleson

Department of Physics

Bachelor of Science

During a critical phase transition there are often dramatic observable effects in the physical properties of a system. These changes are known as critical phenomena and can be seen in many physical systems. One such phenomenon, critical opalescence is characterized by a formerly transparent liquid or gas becoming milky white and opaque at the critical point. It occurs in many systems including a binary fluid system. During this phase, change most physical properties of the system become infinite or go to zero. In a binary fluid mixture, the physical property of interest, optical turbidity, becomes infinite and causes the mixture to turn opaque. This scattering of light allows us to measure the critical exponents of the system. Our goal was to measure the critical exponent  $\gamma$  during a critical phase change of a binary fluid mixture consisting of methanol and cyclohexane. The predicted value of  $\gamma$  is  $1.245 \pm 0.003$  [Le Guillou, J and Zinn-Justin, J. *Phys. Rev. B* **21** 3995]. Unfortunately

our results did not match this same value. Possible explanations and future suggestions for the project are discussed.

## ACKNOWLEDGMENTS

I would like to thank the Ithaca College Physics Department, the H & S Educational Grant Initiative and the National Science Foundation for financial support during this project. I also want to thank Jennifer Mellot for building and rebuilding many essential parts of the experiment. And most importantly I'd like to thank Professor Matthew C. Sullivan my research advisor, for helping me make this project possible, for his instruction on the topic and for his numerous revisions during the editing process.

# Contents

<b>Table of Contents</b>	<b>vii</b>
<b>List of Figures</b>	<b>ix</b>
<b>1 Introduction</b>	<b>1</b>
1.1 Phase Transitions . . . . .	2
1.2 Critical Phenomena . . . . .	6
1.2.1 Fluctuations . . . . .	7
1.2.2 Critical Opalescence . . . . .	8
1.2.3 Critical Exponents . . . . .	9
1.3 Binary Fluid Mixtures . . . . .	11
<b>2 Theory</b>	<b>15</b>
2.1 Using Light to Determine Material Structure . . . . .	15
2.1.1 Bragg Diffraction . . . . .	15
2.1.2 Structure Factor . . . . .	17
2.2 Correlation Function . . . . .	19
2.3 Ornstein-Zernike Theory . . . . .	20
2.4 Turbidity . . . . .	22
2.4.1 Measuring Turbidity . . . . .	22
2.4.2 Deriving Turbidity . . . . .	22
2.4.3 Finding $\gamma$ . . . . .	25
<b>3 Experiment</b>	<b>29</b>
3.1 Binary Fluid Mixture and Optical Cell . . . . .	29
3.2 Temperature Control . . . . .	32
3.2.1 Heating and Insulation . . . . .	32
3.2.2 Temperature Controller . . . . .	34
3.3 Optics . . . . .	35
3.4 Procedure . . . . .	41
3.4.1 Determining the Critical Temperature . . . . .	41
3.4.2 Light Intensity Measurement . . . . .	42

---

<b>4</b>	<b>Data and Analysis</b>	<b>45</b>
4.1	Turbidity . . . . .	45
4.1.1	Cool-down Trials . . . . .	45
4.1.2	Measuring Turbidity . . . . .	48
4.1.3	Critical Exponent $\gamma$ . . . . .	50
4.1.4	Functional Dependence . . . . .	53
<b>5</b>	<b>Conclusion</b>	<b>55</b>
5.1	Future Work . . . . .	57
	<b>Bibliography</b>	<b>58</b>

# List of Figures

1.1	Pressure vs. temperature phase diagram of water . . . . .	3
1.2	Graphs comparing first order and second order phase transitions . . .	5
1.3	Model of fluctuations near a critical phase change . . . . .	8
1.4	Phase diagram of a liquid-vapor transition . . . . .	12
2.1	A simple example of Bragg diffraction . . . . .	16
2.2	Intensity of light scattered from an unknown material . . . . .	17
2.3	Wave vector diagram of light scattering off a single atom . . . . .	18
2.4	Correlation function $G(r)$ . . . . .	21
2.5	Predicted turbidity vs. reduced temperature graph . . . . .	25
2.6	Predicted graph with temperatures close to $T_c$ . . . . .	26
2.7	Predicted graph with temperatures “far” from $T_c$ . . . . .	27
3.1	Optical cell . . . . .	30
3.2	Setup of the tank . . . . .	33
3.3	Setup of the optical equipment . . . . .	36
3.4	Diagram for theory of optics correction factor . . . . .	39
3.5	Approximating $T_c$ from meniscus formation. . . . .	42
4.1	Example of temperature fluctuations affecting data . . . . .	46
4.2	Cool-down rates of various tank setups . . . . .	47
4.3	Intensity ratio of transmitted light vs. temperature graphs of all trials	48
4.4	Intensity ratio vs. temperature graph of four optimum trials . . . . .	49
4.5	$\text{Log}(\tau)$ vs. $\text{log}(T - T_c)$ . . . . .	50
4.6	$\text{Log}(\tau)$ vs. $\text{log}(T - T_c)$ with calculated slopes . . . . .	51
4.7	$\text{Log}(\tau)$ vs. $\text{log}(T - T_c)$ for trial 8 . . . . .	53
4.8	$\tau$ vs. $\ln(T - T_c)$ for trial 8 . . . . .	54



# Chapter 1

## Introduction

Critical opalescence was first witnessed by Thomas Andrews in the liquid-gas transition of carbon dioxide. He gave a lecture on it in 1869 saying,

“On partially liquefying carbonic acid by pressure alone, and gradually raising at the same time the temperature to 88 deg Fahr., the surface of demarcation between the liquid and gas became fainter, lost its curvature, and at last disappeared. The space was then occupied by a homogenous fluid, which exhibited, when the pressure was suddenly diminished or the temperature slightly lowered, a peculiar appearance of moving or flickering striae throughout its entire mass.” [1]

What Andrews observed was carbon dioxide going through a phase transition. There are two different types of phase transitions: first order phase transitions and second order phase transitions. The latter, also known as critical phase transitions, was the phase transition seen by Andrews. A variety of phenomena can occur during these critical phase transitions, and what is described above in Andrews’ experiment is called critical opalescence. In this thesis I will focus on critical opalescence in binary fluid mixtures.

## 1.1 Phase Transitions

In thermodynamics each state of a system is defined by some characteristic energy. If the state of the system is defined by its temperature and its pressure  $T$  and  $P$ , or its temperature and its volume  $T$  and  $V$ , the energy is called the free energy. If the independent variables are the temperature and pressure, then the thermodynamic potential used is the Gibbs free energy,

$$G = E - TS + PV. \quad (1.1)$$

Where  $E$  is the energy of the system at zero temperature and  $S$  is the entropy of the system.

There are two types of phase transitions: first order phase transitions and second order phase transitions. Phase transitions are classified by the order of derivative of the free energy that becomes discontinuous (or in other terms, exhibits singularity) at the phase transition temperature. In first order phase transitions the free energy curve is continuous whereas the first derivative of the free energy, the energy  $E$ , becomes discontinuous.

The most familiar example of a first order phase transition is the phase changes of water [2]. At atmospheric pressure, water is a solid below  $0^\circ\text{C}$ , a gas above  $100^\circ\text{C}$  and a liquid in between. Varying the temperature and the pressure can change water from one phase to another. The lines on Fig. 1.1 are where two phases exist in equilibrium. These are called coexistence curves. The triple point is where all three phases occur simultaneously.

Adding energy to the system will eventually cause a phase transition. For example, if you follow path A in Fig. 1.1 the phase transition occurs because the energy added enables liquid water molecules to escape the attractive forces of other water molecules

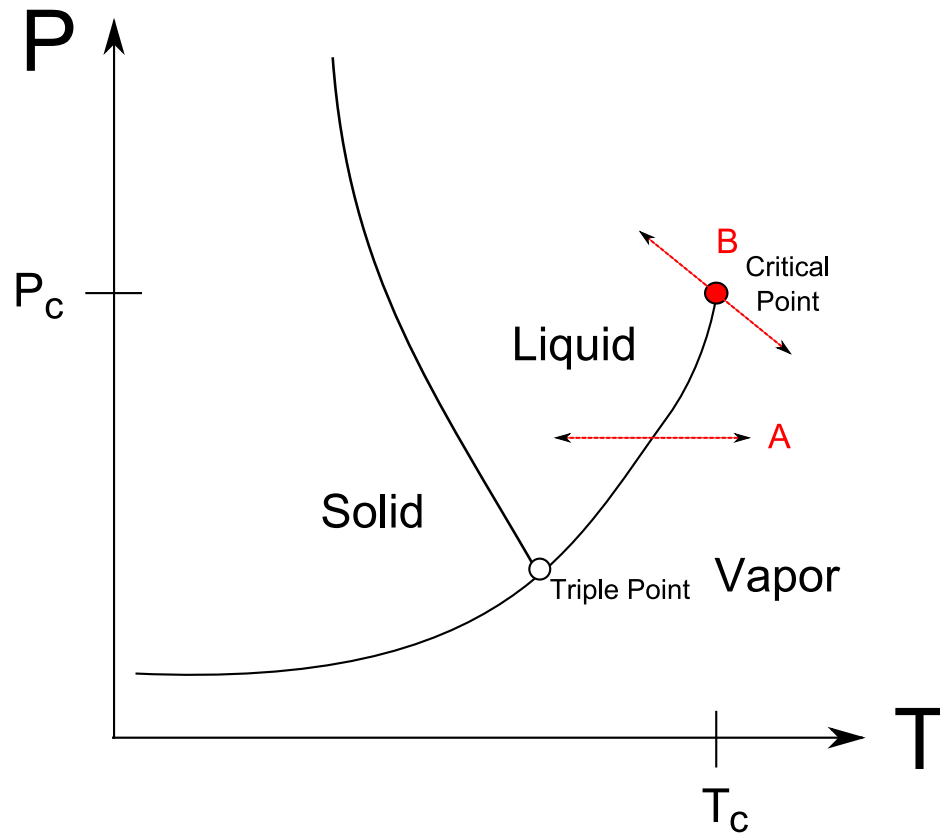


**Figure 1.1** This is an example of a temperature vs. pressure phase diagram. The solid-liquid coexistence curve does not terminate. However, the vapor-liquid coexistence curve terminates at the critical point. Along the dotted line A is a first order phase transition. Along the dotted line B is a second order or critical phase transition.

and they change to a vapor state. This transition occurs at constant temperature. Because the temperature does not change, the energy supplied to the change of state is known as latent heat. [3] This is a first order phase transition because as the liquid converts to a vapor the energy curve with respect to temperature is discontinuous, as shown in Fig. 1.2(a). This discontinuity happens because of latent heat. On the contrary, when passing through the critical point, shown as path B in Fig. 1.1, a second order phase transition occurs.

The fact that the liquid-vapor coexistence curve terminates means that a liquid could be converted to a vapor, or vice versa, continuously, without crossing a coexistence curve. This termination at the end of the coexistence curve is the liquid-vapor critical point. At this point a new, single phase is achieved in which you cannot distinguish the difference between steam and liquid water. At the critical point there is no latent heat and it takes no energy to change phases, therefore the energy vs. temperature curve is continuous, as seen in Fig. 1.2(b). [4] It is called a second order phase transition because during this phase transition there is no latent heat and therefore no discontinuity in the first derivative of the free potential. Other properties corresponding to the *second* derivative of the free energy, such as compressibility and specific heat, *are* discontinuous.

These critical phase transitions can be seen in a wide variety of conditions and systems. In the example given above, temperature and pressure were changed, but other systems have other parameters that are changed: i.e. in ferromagnetism it is the magnetic field and temperature that are manipulated. In the 1960s new theories were introduced regarding these second order phase transitions that made progress possible and the study of them very interesting. [5] Therefore, second order or critical phase transitions are the subject of this study.

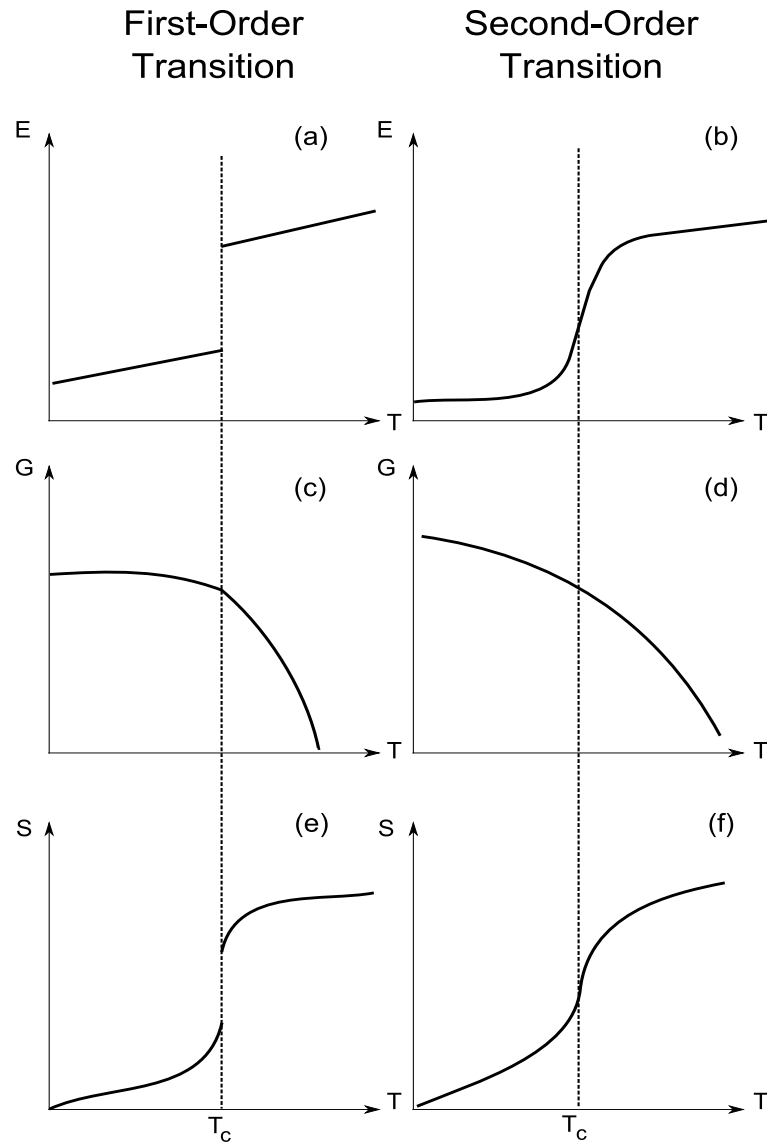


**Figure 1.2** Graphs *a* and *b* show the change in energy with respect to temperature in first and second order phase transitions, respectively. Graphs *c* and *d* show the temperature dependence of the Gibbs potential at a fixed pressure. Graphs *e* and *f* show the entropy obtained from the temperature derivative of the Gibbs potential,  $S = -\left(\frac{\partial G}{\partial T}\right)_P$  [4]. The system undergoes a phase transition at  $T_c$ . In the first order phase transition there is latent heat that can be seen by the discontinuity in the  $E$  vs.  $T$  graph and the  $S$  vs.  $T$  graph. This is not seen in the second order phase transition.

## 1.2 Critical Phenomena

At, or close to the critical point, there are often dramatic observable effects in the physical properties of a system. These changes are known as critical phenomena and many physical systems have phase transitions which exhibit these phenomena.

Transitions in different critical systems can appear to differ from each other in a number of central features. In a gas-liquid system the critical point is at the end of a first order phase transition where the latent heat goes to zero. The phase transition between ferromagnetism and paramagnetism occurs at a certain temperature in zero field. The superfluid transition of helium occurs at a certain temperature called the “lambda point”. Although all of these examples seem different, these diverse transitions are all aspects of the same basic phenomenon.

The phase below the critical point is an ordered phase, meaning it can be characterized by an order parameter that goes to zero at the critical point. The order parameter is normally a quantity which is zero in one phase and non-zero in the other. In fluids, the order parameter is the density difference from the critical density,  $\rho - \rho_c$ . In all cases a response function of the order parameter exhibits a response to an external stress and diverges to zero or infinity at the critical point. This indicates that the system has reached its level of stability [6]. Again in a fluid system, the response function to the order parameter,  $\rho - \rho_c$ , is the derivative of density with respect to pressure. This quantity is proportional to the isothermal compressibility and in binary fluid mixtures the isothermal compressibility becomes infinite. This phenomenon of the response function diverging can be seen in other critical systems. For example, at the ferromagnetic-paramagnetic critical point the magnetic susceptibility becomes infinite and in superconductors the resistivity drops to zero, and conductivity becomes infinite at the critical point. [5].

### 1.2.1 Fluctuations

In all of these examples, energy is not required to switch phases. In all objects there are small variations in energy called fluctuations that vary in size and time [7]. These fluctuations are usually very small and are masked by the statistical approach to thermodynamics. Thermodynamic qualities such as energy in a closed system are thought of as the mean values of all the energies of all the particles in that system. The most probable energy of some portion of the system is  $\bar{E}$ , but it is not always the exact energy of that portion, it is understood that some portions must have fluctuations in which  $E > \bar{E}$  and  $E < \bar{E}$ . [8]

For example, if you take some small subsection of a closed system, it contains an average number of molecules. The density of this subsystem depends on the amount of particles in the specified volume of the subsystem at a given time. If you take smaller and smaller portions, the probability of fluctuations in density increases. These fluctuations do not usually matter, except near the critical point. We discussed that certain physical properties diverge at the critical point. The divergence of these properties causes these fluctuations to become large and dominate the behavior of the system. The system is no longer defined by its thermodynamic qualities but by these fluctuations! [5,8]

Critical point fluctuations are an example of the universality in the relationships between all of these diverse critical systems, meaning it is an example of how all the critical systems (i.e. superconductivity, ferromagnetism, etc.) are related. No additional energy is required to change between phases, and the materials can change phases with fluctuations because there is no latent heat. At or near these various critical points the two phases of these systems coexist and fluctuations control the system [7]. The critical point is different between the various systems, but the physical phenomena describing the systems near the critical point have a universal form and

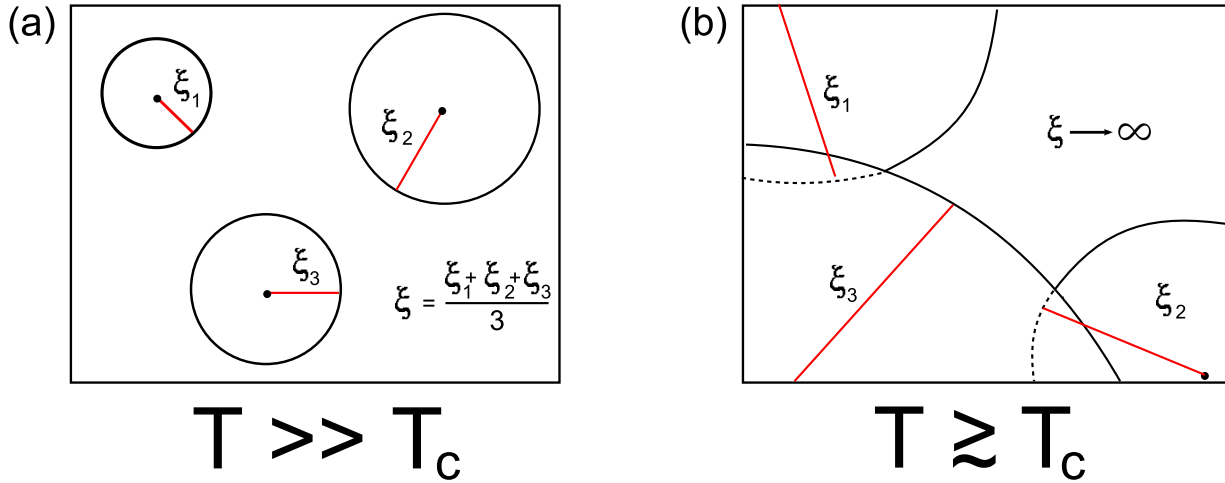


**Figure 1.3** In situation *a* the temperature is much greater than the critical temperature therefore the “droplets” are not interacting as much. In situation *b* the temperature is much closer to the critical temperature causing the “droplets” to overlap and interact and  $\xi$  goes to infinity.

are independent of the systems involved. [5]

## 1.2.2 Critical Opalescence

In fluids, the order parameter that goes to zero at the critical point is the density difference from the critical density,  $\rho - \rho_c$ . When the critical point is approached, the response function diverges and large scale fluctuations in the density can occur with small free energy differences. In order to conceptually understand fluctuations, a “droplets” model can be used. These fluctuations can be seen as the molecules sticking together to form “droplets” that vary in space and time. [9] The average size of these “droplets” is known as the correlation length,  $\xi$ . This can be seen in Fig. 1.3. The correlation length describes the range at which local particle densities are correlated. This means that the state of a material at one point in the material can be predicted accurately using the state of the material at a different point an average distance  $\xi$  away. This will be discussed further in the following chapter. Closer to the critical point,  $\xi$  becomes large, so the droplets become so large that they “stick”

to each other. At the critical point all the “droplets” overlap and interact with each other and  $\xi$  becomes infinite in size [9]. This can be seen in Fig. 1.3(b).

The droplets represent the different states in the material. When their size grows on the order of magnitude of the wavelength of light, it results in the scattering of light. This gives the solution a milky white, opaque appearance. [6] This is known as critical opalescence, and it is one of the more visible and striking examples of the critical phenomena.

### 1.2.3 Critical Exponents

As discussed earlier, a universal property of critical phase transitions is that certain physical properties diverge to zero or infinity. This happens because a response function (magnetic susceptibility, isothermal compressibility, etc) is responding to a change in the order parameter at the critical point. Many of these functions are not measurable and therefore cannot quantitatively describe a system. This is where critical exponents come in. Critical exponents can describe quantitatively the behavior of physical properties at or near the critical point in a system. They are independent of the system and therefore do not depend on the details of the physical properties of the system. Because of this, they are universal and can be used to describe any system [5].

To explain how critical exponents are independent of the system we can start with a general definition of a critical exponent. We begin with the general response function  $f(t)$ , where,

$$t \equiv |T - T_c|, \quad (1.2)$$

a dimensionless variable that measures the difference in temperature from the critical temperature. We want to describe the behavior of a physical quantity,  $f(t)$  with a

power law dependence. So if we write,

$$f(t) \sim t^\lambda, \quad (1.3)$$

we mean that the function  $f(t)$  goes as  $t$  to  $\lambda$ . At the critical point  $t, T \rightarrow T_c$  so  $t \rightarrow 0$ . Thus by Eq. 1.3 we can describe  $\lambda$  as,

$$\lambda \equiv \lim_{t \rightarrow 0} \frac{\log f(t)}{\log(t)}. \quad (1.4)$$

$\lambda$  is still a critical exponent of  $f(t)$  even if other constants define this function. Eq. 1.3 does not mean  $f(t) = Ct^\lambda$ . In general, in thermodynamics functions usually have correction terms and are more complicated. For example, it is more likely that,

$$f(t) = t^\lambda(1 + At^\lambda + \dots). \quad (1.5)$$

At the critical point the function diverges, as  $t \rightarrow 0$ ,  $f(t) \rightarrow 0$  if  $\lambda > 0$  or,  $f(t) \rightarrow \infty$  if  $\lambda < 0$ . Therefore, near the critical point the behavior of the leading term dominates and we can ignore the rest of the terms.

We study critical exponents because they are usually experimentally measurable, while the complete function may not be. They describe the rate at which these systems become singular (diverge either to zero or infinity). There are also a large number of other relations between these exponents that are applicable to many varieties of systems [4].

Consider the following exponent  $\gamma$ . It is defined by

$$K_T \sim t^{-\gamma}, \quad (1.6)$$

where  $K_T$  is known as the isothermal compressibility. In binary fluid mixtures, when the critical point is reached the isothermal compressibility diverges to infinity. The critical exponent  $\gamma$  describes how fast this quantity diverges. In the critical phenomenon known as critical opalescence, turbidity depends on  $K_T$ . This diverges close to the critical point with a power law dependence on the critical exponent  $\gamma$ .

### 1.3 Binary Fluid Mixtures

Critical opalescence can be seen in binary fluid mixtures. A binary fluid mixture is a mixture with two components that are partially miscible (soluble) below a certain temperature,  $T_c$ , and completely miscible above [9]. For temperatures below  $T_c(\rho)$ , the compositions of two liquids, A and B, will result in two immiscible (or partially miscible) phases. Each phase will actually be a solution, one will be a solution of A in B and the other will be a solution of B in A, i.e., the role of solvent and solute will be reversed. For temperatures above  $T_c$ , thermal motion overcomes the tendency for phase separation at all compositions and so the system is a homogenous mix of both liquids A and B. Consequently, at  $T_c$ , the two phase system (solutions of A in B and B in A) and the one phase system (homogenous mix of A and B) coexists with strong concentration fluctuations between the two phases. [10]

The behavior of binary fluid mixtures is closely analogous to the liquid-vapor phase transition and can be explained according to a simple fluid model. [11] Fig. 1.4 is a simple example of a graph showing how temperature and pressure affect the state of a liquid-vapor phase transition. Below the critical temperature, the two phases are separated. However, above the critical temperature the liquid and vapor phases coexist without any distinction between the two.

The transition from a one phase solution to a two phase solution is called a spin-

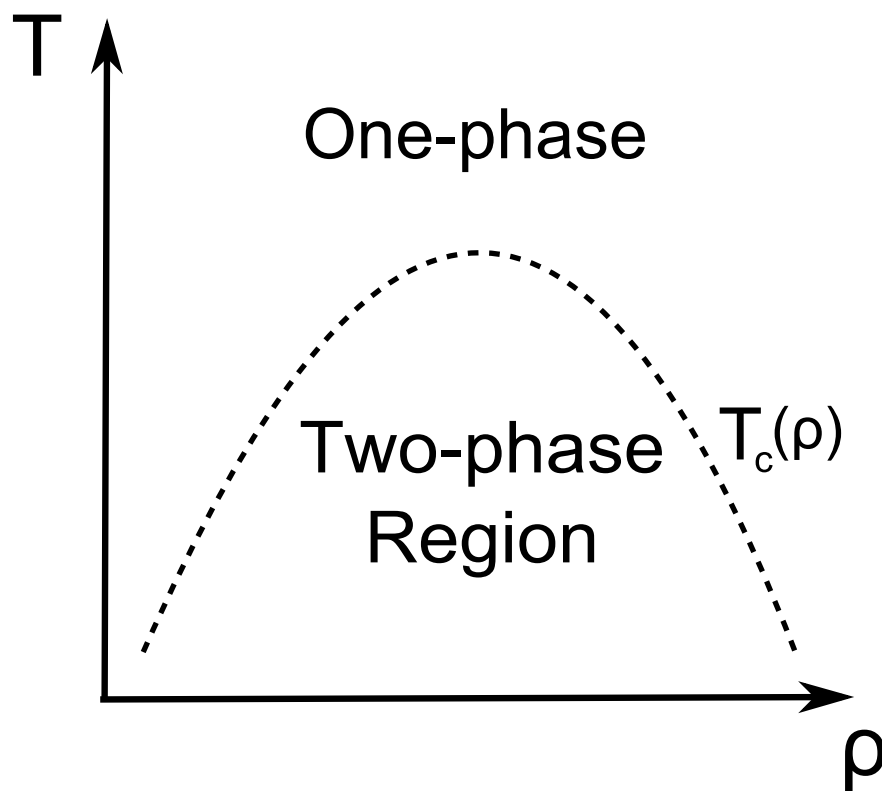


**Figure 1.4** A binary fluid mixture is analogous to the phase transition of a simple fluid. Above a critical temperature the liquid and vapor phases coexist as one single phase. Below the critical temperature they are in two separate phases.

odal decomposition, and is characterized by the strong scattering of light, critical opalescence. [12] The binary fluid mixture of methanol and cyclohexane exhibits this phenomenon. When the methanol-cyclohexane solution is at a high temperature above the critical point it is a one-phase solution and below the critical temperature it is a two-phase solution. [13] Methanol and cyclohexane make up the binary fluid mixture I use in my experiment.

Methanol and cyclohexane make a good binary fluid mixture for critical phase transitions because of the physical properties of their molecules. Methanol consists of a carbon atom with three hydrogen atoms, attached to an oxygen atom with a hydrogen atom. Cyclohexane is a 6 member carbon ring with two hydrogen atoms attached to each carbon. Oxygen is a highly electronegative atom and therefore a small dipole is created between the carbon and oxygen in methanol. Acting on both molecules are van der Waals forces that cause the molecules to want to form brief bonds with each other. However, because methanol forms a dipole, the slightly more negative oxygen is going to be more attracted to the slightly more positive carbons of other methanol molecules. So at low temperatures, the large and neutral cyclohexane molecule cannot mix very well with the methanol molecules. However, as temperature increases the motion and energy of the molecules supersede that of the dipole bonds between methanol molecules. This allows cyclohexane and methanol to mix more readily.



# Chapter 2

## Theory

In order to find the value for the critical exponent  $\gamma$ , we need to utilize several properties of the materials in this two-state system. To describe light scattering during critical opalescence, we use the structure factor and the correlation function of the fluid system. The structure factor of a material describes how light is scattered from that material. The correlation function of a system measures the extent to which two particles, separated by a distance  $\vec{r}$  are correlated [6]. The Fourier transform of the correlation function gives us the structure factor. In this chapter I will elaborate on these properties and describe how these functions near the critical point for a binary fluid system can be used to determine the value for  $\gamma$ .

### 2.1 Using Light to Determine Material Structure

#### 2.1.1 Bragg Diffraction

Determining the atomic structure of a material is very difficult and it cannot be done simply by putting a material under an optical microscope. However, it was discovered at the beginning of the last century that light of non-visible wavelengths can be used

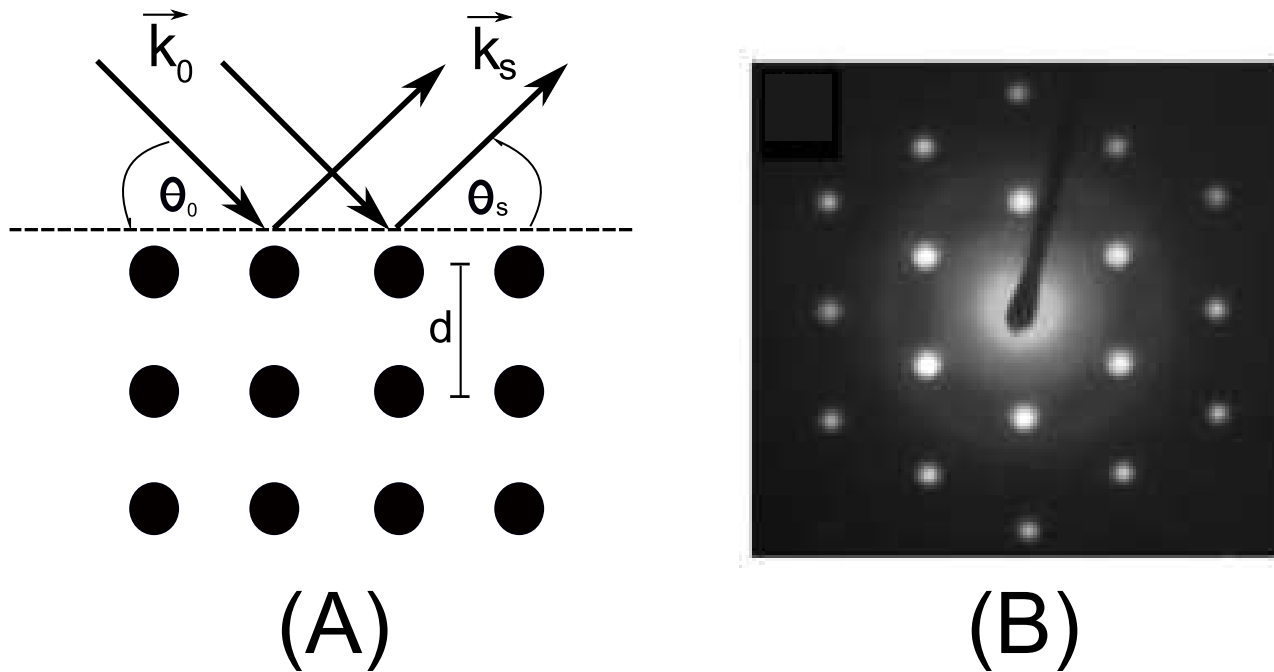


**Figure 2.1** This is a simple example of Bragg diffraction on a 2D rectangular array. As light reflects off the atoms the scattered beams constructively and destructively interfere depending on their path differences and creates a pattern seen on the right [15].

instead. In 1912, x-ray diffraction was used to determine the structure of crystals. [14] X-ray diffraction occurs when electromagnetic radiation with a wavelength on the same scale as the spacings between adjacent atoms ( $\approx 1 - 10$  Angstroms) is incident upon a crystalline sample. The scattered light reflected from the crystalline sample undergoes interference and makes patterns that are representative of specific atomic configurations [14]. A sketch of light hitting a rectangular array of atoms can be seen in Fig. 2.1(A) and an example of the resulting diffraction pattern can be seen in Fig. 2.1(B).

The resulting diffraction pattern depends on the wavelength of the radiation  $\lambda$ , the angle at which it hits the atom  $\theta$ , and the distance  $d$  between the atoms [14]. These patterns were first analyzed by Sir William Bragg and his son Laurence Bragg and thus the phenomenon is known as Bragg diffraction. [14]

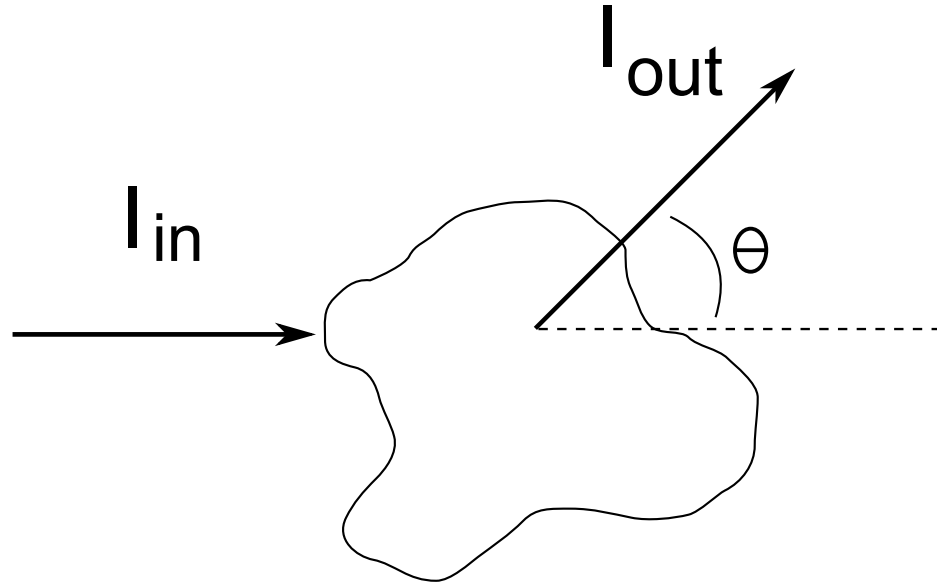


**Figure 2.2** The intensity of light scattered from an unknown material. Examining  $I_{out}$  as a function of angle can tell us how the material is structured.

### 2.1.2 Structure Factor

We can generalize this type of study to other materials and objects. The way to describe how light will scatter off of a material is by using a function called the structure factor. We just discussed x-ray diffraction, which is a technique that uses this principle to examine the structure of a crystalline solid [5]. However, the structure factor can be used to describe any material, not only crystalline structures. An example is shown in Fig. 2.2. Examining  $I_{out}$  as a function of angle can tell us how the material is structured. For solids, the structure factor is easy to define because it is a periodic array of atoms in space. However for a liquid, the structure factor cannot be defined so clearly.

For the structure factor, it is easier to discuss the light not in terms of wavelength, but as wave numbers. The energy of light can be written in several different ways. Some examples are,

$$E_{light} = h\nu = pc = \hbar kc = \frac{hc}{\lambda}. \quad (2.1)$$

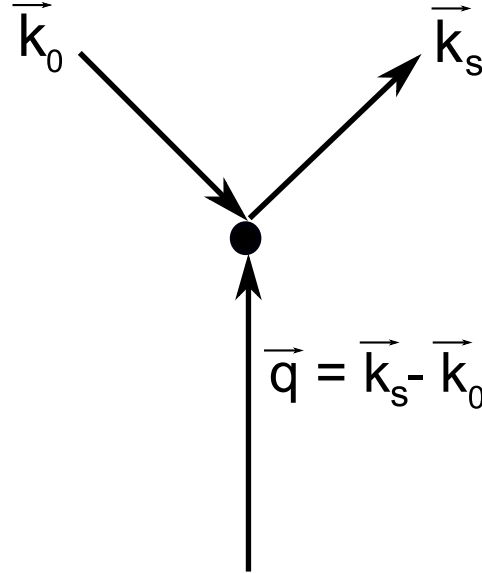


**Figure 2.3** This is a wave vector diagram from one incident beam reflecting off of an atom, resulting in a scattered beam. The momentum transferred from the material is labeled  $\vec{q}$ .

The wave number  $k$  is given by  $k = \frac{2\pi}{\lambda}$ , and can be thought of as momentum that is off by a factor of  $\hbar$ . In Fig. 2.3, wave numbers are used to illustrate the change in momentum from the incident and transmitted beams after the incident beam is scattered off one atom from the 2D rectangular array previously seen in Fig. 2.1(A).  $\vec{k}_0$  is the incident wave number vector and  $\vec{k}_s$  is the scattered wave number vector. The difference between these two vectors is the momentum transferred from the crystalline structure to the light causing it to scatter at certain angles. The momentum  $\vec{q}$  that is transferred to the light depends on the material. Therefore, light will scatter differently when incident upon different materials.

A general equation for the intensity of the scattered light is,

$$I_{out}(\vec{q}) \sim \frac{1}{\rho} S(\vec{q}) \quad (2.2)$$

where  $S(\vec{q})$  is the structure factor and  $\rho$  is the density of a material [5]. The structure

factor and therefore the intensity is a function of the momentum (wave number) that the material can give to the light. The structure factor will become relevant in the subsequent section of the theory.

## 2.2 Correlation Function

The correlation function predicts the state of a material at one point with respect to the state of the material at a different point. For example, if I know what the state of the material is at  $\vec{r}$ , and the material is highly correlated, then I know what the material is at  $\vec{r}'$ . The general formula for the correlation function is [4],

$$G(\vec{r} - \vec{r}') = \langle \rho(\vec{r})\rho(\vec{r}') \rangle - \bar{\rho}^2. \quad (2.3)$$

If  $\rho(\vec{r})$  and  $\rho(\vec{r}')$  do not affect each other, they are not correlated, and  $\langle \rho(\vec{r})\rho(\vec{r}') \rangle$  becomes  $\bar{\rho}^2$  and thus  $G(\vec{r} - \vec{r}') = 0$  [5].

In this equation, I use  $\rho$  because it is easy to discuss the correlation function in terms of density. Note however, that the correlation function can be used for a variety of physical parameters: spin, phase etc. [5] In my experiment I am working with binary fluid mixtures. This means for my experiment, a possible state of the material is the two phase state: in this state, the separation between the two liquids is distinct. The other possible state of the material is the one phase state: in this state, the two liquids are mixed. For my experiment, when examining two locations a distance  $\vec{r}$  away, the correlation function predicts the likelihood of the material at these two locations being in the same state: e.g., both locations being in the two phase state. Conversely, the correlation function predicts the likelihood that two points separated by a distance  $\vec{r}$  will be in different states, e.g. a mixed state at the origin and a two phase state at  $\vec{r}$ .

The correlation function helps because when we go from momentum space to physical space we can take the Fourier transform of the structure factor,  $S(\vec{q})$ ,

$$\int e^{(+i\vec{q}\cdot\vec{r})} S(\vec{q}) \frac{d^3\vec{q}}{(2\pi)^3} = G(\vec{r}) \quad (2.4)$$

and the result is the correlation function,  $G(\vec{r})$  [5].

As stated previously, a crystalline structure is highly ordered and therefore the structure factor can be determined. However, in liquids we cannot find  $S(\vec{q})$  directly. Therefore, taking the Fourier transform of  $S(\vec{q})$ , which we do not know, would be quite difficult. In order to predict what the structure factor is and subsequently what the correlation function is, we must rely on physical models. One of the simplest and most successful models is Ornstein-Zernike Theory.

## 2.3 Ornstein-Zernike Theory

To simplify things let us take  $\vec{r} = 0$  and therefore  $|\vec{r} - \vec{r}'| \equiv r$ . It can be shown that for binary fluids, using the inverse Fourier transform of the structure factor as predicted by Ornstein-Zernike theory, the correlation function will be given by [5]

$$G(r) \sim \frac{e^{-\frac{r}{\xi}}}{r}. \quad (2.5)$$

For a location far from the origin, the particles are not correlated,  $G(r) \rightarrow 0$  as  $r \rightarrow \infty$ . This can be seen in Fig. 2.4. The distance  $\xi$  is called the correlation length. It describes the average distance in space you can go and the material will remain in the same state. Alternatively,  $\xi$  describes the range of interaction between two particles [6].

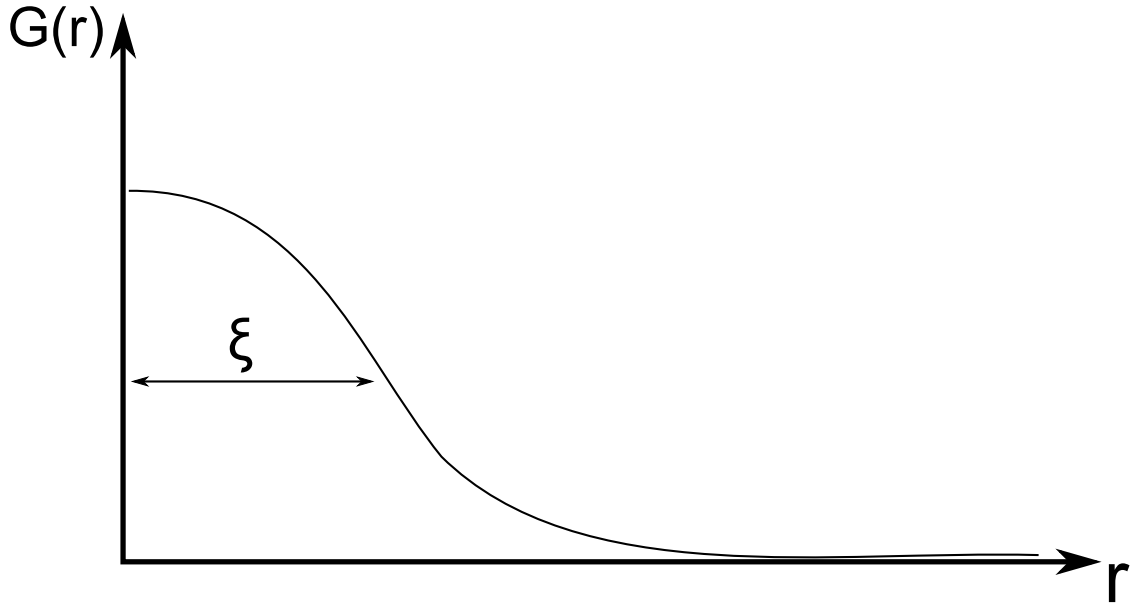


**Figure 2.4** This is a sketch of the correlation function  $G(r)$ . As  $r \rightarrow \infty$ , meaning the distance between two points increases,  $G(r) \rightarrow 0$ . This means at this point you cannot know what the phase of the material.

The size of the correlation length varies with temperature according to

$$\xi = \xi_0 |T - T_c|^{-\nu}, \quad (2.6)$$

where  $\xi_0$  is the correlation length at  $T = 0$  [9, 16]. Near the critical point there are large scale fluctuations between the two different states of the material, in our case, mixed liquids or separated liquids. The average length of these fluctuations in the material is  $\xi$  as discussed earlier. When  $T = T_c$ ,  $\xi \rightarrow \infty$ , meaning the material is infinitely correlated. As  $T$  approaches  $T_c$ ,  $\xi$  gets larger and larger. Light scatters because the size of  $\xi$  gets so large that it is on the same order of magnitude as the wavelength of light.

## 2.4 Turbidity

### 2.4.1 Measuring Turbidity

Turbidity is defined as the total incremental intensity of light scattered per unit length and is denoted by  $\tau$ . When the binary fluid mixture is in one homogenous phase the mixture is clear and the intensity of the transmitted light is  $I_0$ . When the temperature approaches  $T_c$ , the fluctuations start and the transmitted light,  $I$ , decreases. The intensity of the transmitted light is given by,

$$I = I_0 \exp^{-\tau L}, \quad (2.7)$$

where  $L$  is the optical path length [16]. Therefore the equation for turbidity,  $\tau$ , is,

$$\tau = -\frac{1}{L} \ln \left( \frac{I}{I_0} \right) \quad (2.8)$$

### 2.4.2 Deriving Turbidity

From Ornstein-Zernike theory, the light-scattering intensity per unit length is [9,16,17]

$$I(q) = A t^{-\gamma} \frac{\sin^2 \Phi}{1 + (q\xi)^2}, \quad (2.9)$$

where  $A$  is a constant that depends on the wavelength of light, the index of refraction of the material, and the osmotic susceptibility [18],  $t$  is the reduced temperature  $t = |T - T_c|$ ,  $q = |\vec{k}_0 - \vec{k}_s| = \frac{4n\pi}{\lambda} \sin(\theta/2)$  is the scattering wave vector,  $\Phi$  is the angle between the polarization vector of the incident beam and the scattering wave vector, and  $\xi$  is the correlation length. The turbidity can be found by taking the integral over all angles of this light-scattering intensity per unit length [16].

After integrating over all angles, Eq. 2.9 becomes

$$\tau = \tau_0 t^{-\gamma} (2a^2 + 2a + 1) \frac{[\ln(1 + 2a)]}{a^3} - \frac{2(1 + a)}{a^2}, \quad (2.10)$$

where  $a = 2q_0^2 \xi^2$ ,  $q_0 = \frac{2\pi}{\lambda}$ ,  $\xi$  is the correlation length, and  $\tau_0 = A\pi$ . [16] If you consider

$$f(a) = (2a^2 + 2a + 1) \frac{[\ln(1 + 2a)]}{a^3} - \frac{2(1 + a)}{a^2}, \quad (2.11)$$

then Eq. 2.10 becomes

$$\tau = \tau_0 t^{-\gamma} f(a). \quad (2.12)$$

Let us recall Eq. 2.6,

$$\xi = \xi_0 |T - T_c|^{-\nu}, \quad (\nu > 0). \quad (2.13)$$

From Eq. 2.6 we can see that when  $T \gg T_c$ ,  $\xi$  becomes small. And thus, when  $T \gg T_c$ ,  $a$  also becomes small. Now when  $T \rightarrow T_c$ ,  $\xi$  becomes large and so  $a$  becomes large. Keeping this in mind we can predict the behavior of turbidity at certain temperatures near  $T_c$ . The behavior of the turbidity in the phase transition ( $T \approx T_c$ ) can be approximated under two conditions: when it's "far" above  $T_c$ , and when its very close to, yet still above,  $T_c$ .

When the temperature is "far" above  $T_c$ , we take the limit of Eq. 2.11 as  $a \rightarrow 0$ . [9] Using L'Hopital's rule,  $f(a)$  becomes a constant.

$$\lim_{a \rightarrow 0} f(a) = \frac{8}{3} \quad (2.14)$$

Therefore Eq. 2.12 becomes

$$\tau = \frac{8}{3} \tau_0 t^{-\gamma}. \quad (2.15)$$

Now we'll consider the other condition in which we can approximate the behavior

of the turbidity: when the temperature is very close to but above  $T_c$ . At this point,  $T \rightarrow T_c$ , which results in  $(T - T_c)$  being very small. Thus,  $|T - T_c|^{-\nu}$  is very large. So according to Eq. 2.6, when  $T \rightarrow T_c$ ,  $\xi \rightarrow \infty$ , and thus  $a \rightarrow \infty$ . Therefore taking the limit of Eq. 2.11 as  $a \rightarrow \infty$  results in,

$$f(a) \rightarrow \frac{2}{a} \ln(1 + 2a) \approx \frac{2}{a} \ln(2a), \quad (2a \gg 1) \quad (2.16)$$

and Eq. 2.12 becomes, [9]

$$\tau = \tau_0 t^{-\gamma} \frac{2}{a} \ln(2a). \quad (2.17)$$

Now we know,  $a = 2q_0^2 \xi^2 = 2q_0^2 \xi_0^2 |T - T_c|^{-2\nu} = 2q_0^2 \xi_0^2 t^{-2\nu}$ . Therefore Eq. 2.17 becomes,

$$\tau = \left( \frac{\tau_0 t^{-\gamma+2\nu}}{q_0^2 \xi_0^2} \right) \ln(2a). \quad (2.18)$$

However,  $\nu = \frac{\gamma}{2}$ , so  $-\gamma + 2\nu = 0!$  [19] So Eq. 2.18 becomes

$$\tau = \left( \frac{ta u_0}{q_0^2 \xi_0^2} \right) \ln(2a) = \left( \frac{\tau_0}{q_0^2 \xi_0^2} \right) \ln(4q_0^2 \xi_0^2 t^{-2\nu}). \quad (2.19)$$

And then substituting in the values for  $a$  and  $t$ ,  $\xi$  Eq. 2.19 becomes,

$$\tau = \left( \frac{\tau_0}{q_0^2 \xi_0^2} \right) [\ln(4q_0^2 \xi_0^2) - 2\nu \ln |T - T_c|]. \quad (2.20)$$

To simplify Eq. 2.20 we can group the constant terms together and rename them so that  $B = \ln(4q_0^2 \xi_0^2)$  and  $A = \left( \frac{\tau_0}{q_0^2 \xi_0^2} \right)$ . [9] This yields,

$$\tau = BA - 2B\nu \ln |T - T_c|. \quad (2.21)$$

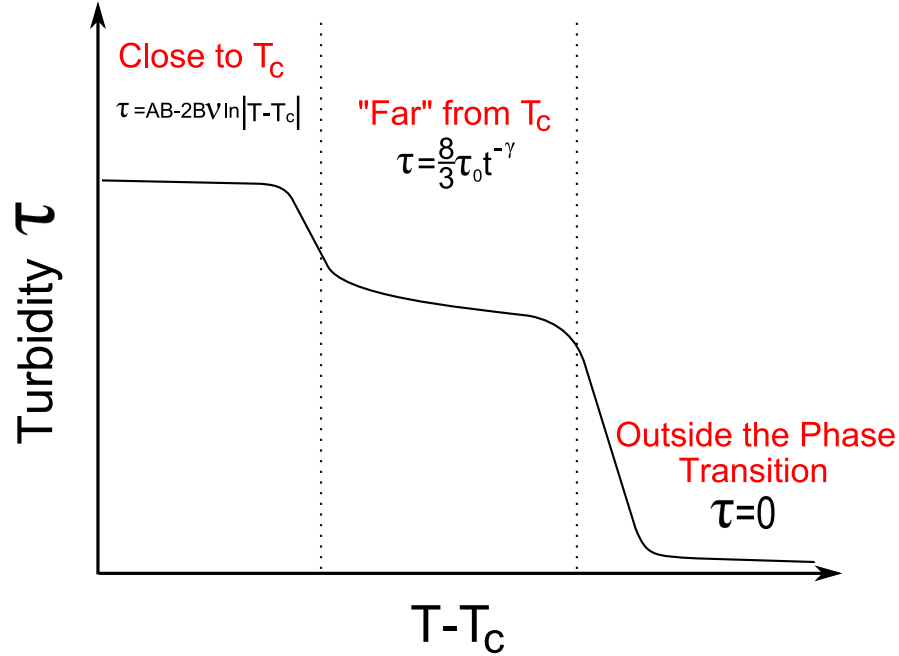


**Figure 2.5** This is an example of a turbidity vs. reduced temperature graph. This graph highlights three regions. The region furthest to the left is ( $T - T_c = 0$ ). In this section turbidity follows Eq. 2.21. The middle region is “far” from  $T_c$  and it follows Eq. 2.15. The region furthest to the right is very far from  $T_c$  where the turbidity is zero.

### 2.4.3 Finding $\gamma$

In the previous section we arrived at two very important conclusions regarding  $\tau$ , the turbidity. At temperatures “far” away from  $T_c$ , turbidity follows the behavior of Eq. 2.15,  $\tau = \frac{8}{3}\tau_0 t^{-\gamma}$ . And when temperatures are very close to  $T_c$ , turbidity follows the behavior of Eq. 2.21,  $\tau = BA - 2B\nu \ln|T - T_c|$ . An example of a graph that depicts these behaviors can be seen in Fig. 2.5.

If we only consider temperatures close to  $T_c$ , then the graph of Eq. 2.21 would yield a straight line with a negative slope shown in Fig. 2.6. However, we don’t know the the values of  $A$  and  $B$  in Eq. 2.21, so we can only see that the equation does yield a straight line with a negative slope, but we do not know anything about the line (i.e. slope, y-intercept).

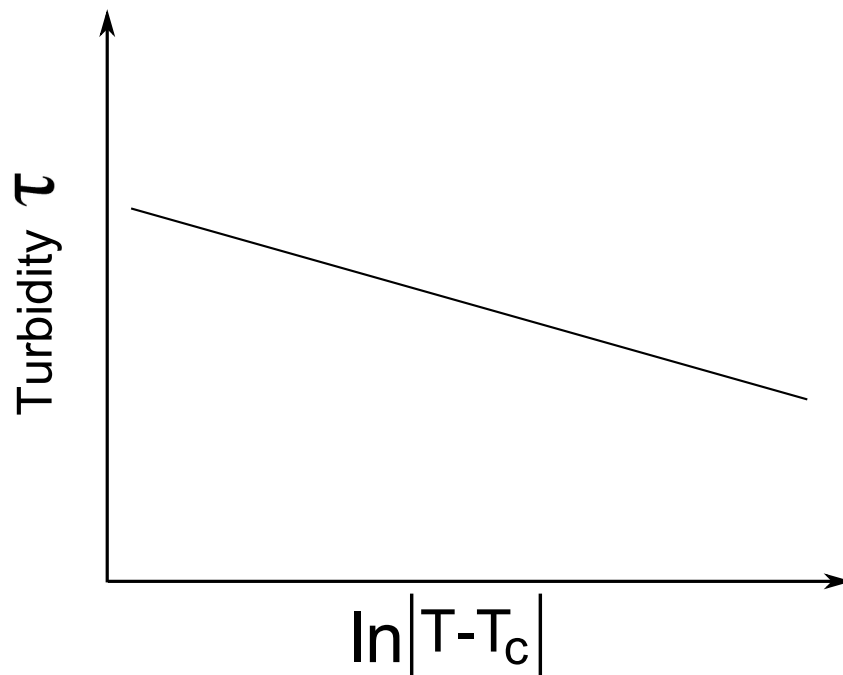


**Figure 2.6** This is an example of what a graph would look like following the behavior of turbidity when only considering temperatures very close to  $T_c$ . However, we don't know the the values of  $A$  and  $B$  in Eq. 2.21, so we can only see that the equation does yield a straight line with a negative slope, but we do not know anything about the slope or intercept of the line.

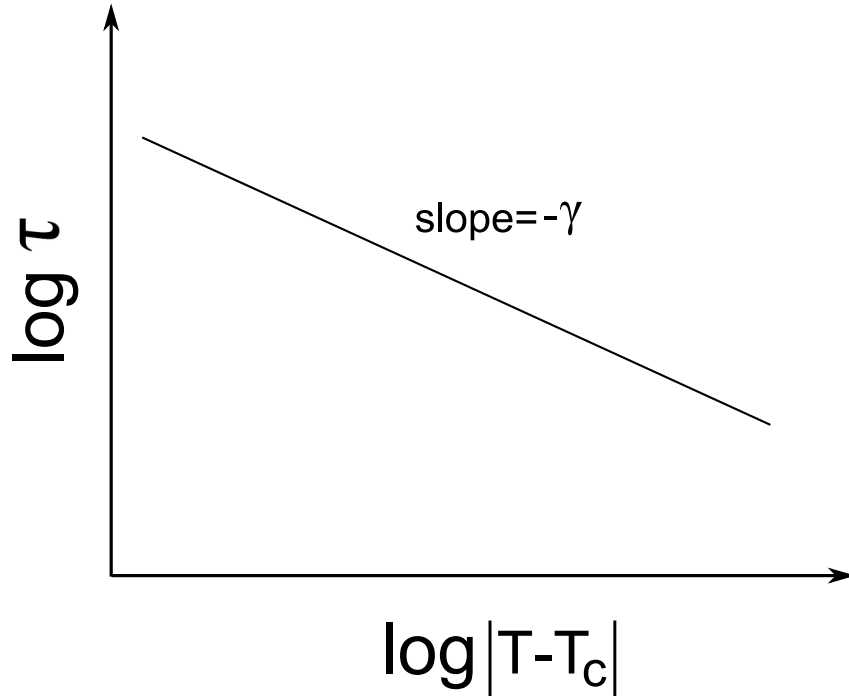


**Figure 2.7** This is an example of what a graph would look like following the behavior of turbidity when only considering temperatures “far” from  $T_c$ . By taking the logarithm of both sides of Eq. 2.15 and graphing it, the result is a straight line with a slope of  $-\gamma$ .

However, we are trying to figure out the value for  $\gamma$ . To do this we are going to use Eq. 2.15, where we only consider the behavior of the turbidity at temperatures “far” from  $T_c$ . If we take the logarithm of both sides of Eq. 2.15 and rearrange the equation using the rules of logarithms we get,

$$\log(\tau) = \log\left(\frac{8}{3}\tau_0\right) - \gamma \log |T - T_c|. \quad (2.22)$$

Since  $\tau_0$  and  $C$  are just constants, graphing Eq. 2.22 will yield a straight line with a slope of  $\gamma$ ! [9]. This can be seen in Fig. 2.7. The theoretical value for  $\gamma$  is  $1.245 \pm 0.003$  [20].



# Chapter 3

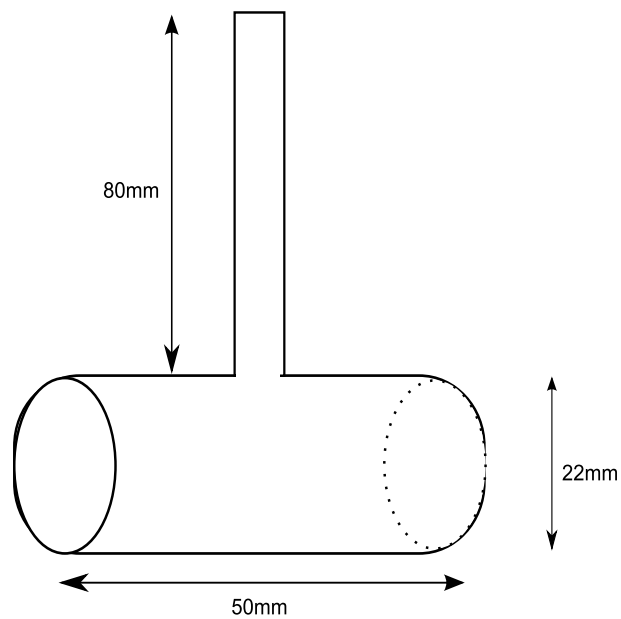
## Experiment

This experiment has several major components: the cell containing the binary fluid mixture, temperature control surrounding the cell, and the optical system that takes the light intensity measurements. In this section I will describe how each component is set up and how they are each used in the experimental procedure.

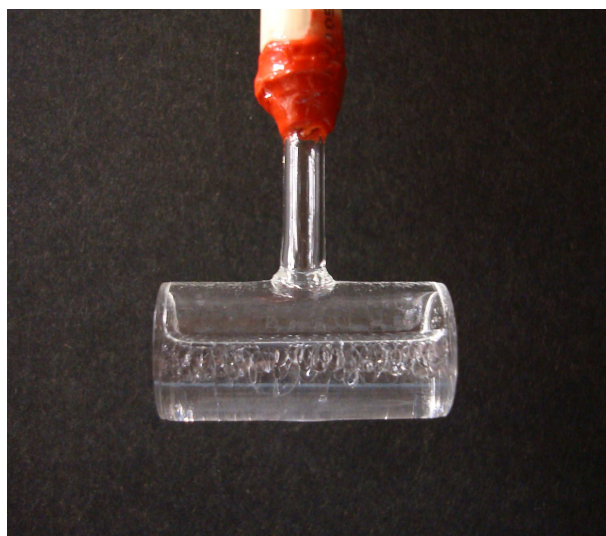
### 3.1 Binary Fluid Mixture and Optical Cell

The binary fluid mixture in the cell is made up of 4 mL of methanol and 4 mL of cyclohexane because the critical composition by volume for a methanol cyclohexane mixture is approximately 51.65% methanol [21]. We use these two liquids for the experiment because they can be brought together at room temperature and atmospheric pressure. Also the mixture has partial miscibility, meaning that below  $T_c$ , the two fluids cannot mix and they form two distinct mixtures. However, above  $T_c$  the two liquids form one uniform mixture. These conditions allow a phase transition at  $T_c$  needed for the experiment.

The binary fluid mixture is held in an optical cell. The optical cell can be seen in



(a) Diagram of Cell



(b) Photo of Cell

**Figure 3.1** Inset (a) is a sketch of our optical cell, and (b) is a photo of the optical cell. The two flat circles are the optical windows. The laser path is through these optical windows. The cell holds 15 mL of solution. The top tube is sealed using a torch.

Fig. 3.1. The cell has two optically flat windows on its flat edges perpendicular to the length of the cell. During the experiment, the laser passes through these windows. The cell is sealed under vacuum to prevent interactions with the atmosphere and any air that would be inside the tube. For example, convection inside the tube would not allow a precise measurement of the temperature of the solution.

Before we sealed the glass tube on top of the cell we put the 8 mL solution inside the cell and froze the mixture. Both fluids are flammable and can ignite during the sealing process, and we froze them in order to prevent this. Also before sealing the cell, we de-gassed the solution. To do this we freeze the solution, evacuate it, let it melt so all the gas is released and repeat the process. This process forces any carbon dioxide already in the two liquids to emerge and be removed. This process of freeze-pumping the fluid is also helpful because it decreases the pressure inside the cell. After the cell is sealed, the solutions melt and release any gas they had mixed with them. These gases create pressure on the newly sealed cell and if there is an excess of carbon dioxide, it could break open the seal.

Once the solution is prepared, a torch line is used to seal the glass tube on top of the cell. During our first trial we used liquid nitrogen to freeze the two solutions. The freezing point of methanol is  $-97^{\circ}\text{C}$ , and the freezing point of cyclohexane is  $6.5^{\circ}\text{C}$ . Therefore, liquid nitrogen at  $-196^{\circ}\text{C}$  would freeze both liquids. [22] However, after the cell was sealed and left at room temperature to melt, the cell endured too much thermal stress and one of the optical windows unsealed from the cell and broke off. Therefore for the second trial, we alleviated as much stress on the cell as possible. We did not go as drastically low in temperature, and we did not freeze pump the sample to de-gas it. Instead we used a mixture of acetone and dry ice to cool the sample. The dry ice solution was at  $-56.4^{\circ}\text{C}$  so only the cyclohexane freezes, but we were still able to cool down the methanol so that it did not catch fire under the torch. This

method was less stressful for the cell and was successful.

Once the sample is sealed it is attached to a PVC pipe by silicon high temperature glue. This is done so that the cell could be taken in and out of the tank and suspended conveniently with a clamp. We use high temperature glue because the cell is placed in temperatures at  $\approx 55^\circ\text{C}$ .

## 3.2 Temperature Control

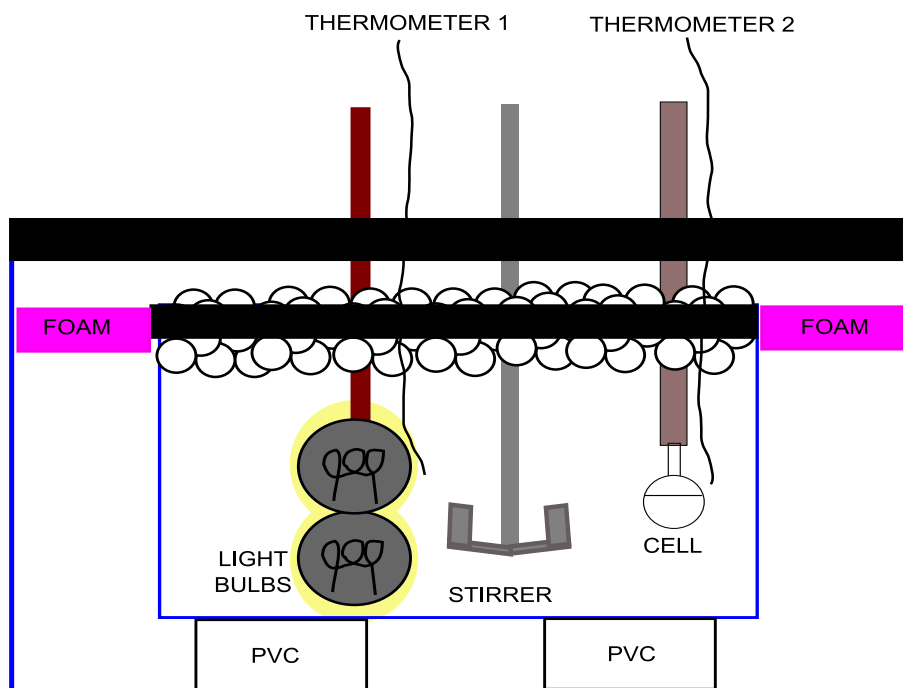
Temperature control is a crucial part of the experiment. The goal of the experiment is to measure turbidity, which has a power law dependence on the difference between the cell temperature and the critical temperature. Therefore it is necessary to get as close to the critical temperature as possible ( $\pm 0.001^\circ\text{C}$ ) at a slow, steady rate.

### 3.2.1 Heating and Insulation

To heat and insulate the cell it is placed in a small fish tank filled with mineral oil. Mineral oil is used because the heating source in the tank is two light bulbs and mineral oil does not pose a threat of conducting electricity. Also, mineral oil will not evaporate. Light bulbs are used because they are a convenient and accurate way to make small changes in temperature. The light bulbs are painted black so that their light does not interfere with any measurements, and because black absorbs and re-radiates heat better.

To achieve a uniform temperature throughout the tank, a stirrer is also placed inside. The stirrer is made of aluminum fins attached to a pole and is spun by a drill. The drill is connected to a variable AC source so that its speed is regulated and can be changed. A sketch and a photograph of the tank can be seen in Fig. 3.2.

This small fish tank is put on top of cross-sections of PVC and placed inside a



(a) Diagram of Tank



(b) Photo of Tank

**Figure 3.2** This is a front view of the tank set up. Inset (a) is a sketch and inset (b) is a photo of the tank. The smaller tank holds the mineral oil, cell, light bulbs and stirrer. It is inside the larger tank and is further insulated with foam and polystyrene balls.

larger fish tank. Foam is placed around the rim of the small tank to insulate the air in between the tanks. Small 10 mm diameter polystyrene balls are placed on top of the small fish tank. They insulate the top of the fish tank while allowing easy movement of the equipment inside the tank if it is necessary. All of these insulating measures are taken so the temperature in the tank holding the cell is kept constant and does not interact with the ambient temperature in the room. Two thermometers are placed in the tank; one near the heat source and one near the cell.

### 3.2.2 Temperature Controller

The thermometer near the light bulbs is connected to a PID temperature controller. A PID temperature controller is a proportional-integral-derivative controller that uses a feedback mechanism to control the temperature. It calculates the difference from the current temperature to the desired set point temperature and adjusts its power output accordingly. We set the temperature controller to 60°C. It reads the temperature of the tank and adjusts the power output of the light bulbs. We used this temperature controller to decrease the temperature of the tank very slowly and uniformly.

To achieve a consistent temperature, the P(proportional), I(integral), and D(derivative) coefficients must be changed for each unique system. The first step in this process is to find a P coefficient that oscillates about the set point temperature. From the period and amplitude of these oscillations the I and the D coefficient can be calculated. However in our system, the stirrer creates tiny temperature variations. These variations are read by the controller and the power output of the controller is very inconsistent and noisy. We were unable to achieve temperature stability using the PID controller.

We could not eliminate the stirrer because without it, the temperature gradient across the tank is too great and the temperature around the cell is not uniform.

We used the temperature controller to monitor the temperature and to adjust the power output of the light bulbs manually. Because we could not control the temperature, we decided to cool the tank down very, very slowly while taking light intensity measurements.

Upon taking data to determine the critical exponent  $\gamma$ , we realized that the small fluctuations in temperature caused by the stirrer had a not unsubstantial effect on the intensity measurements. Therefore, we had to determine the best scenario in which to cool down the tank slowly, while eliminating these temperature fluctuations. We ended up keeping the light bulbs on at 25% power, and turned off the stirrer. The steps that led to this conclusion as well as an analysis of the different cooldown rates will be discussed in Ch. 4.

### 3.3 Optics

The optical system that we used can be seen in Fig. 3.3. This experiment uses a HeNe laser that provides a monochromatic beam at  $\lambda = 533\text{nm}$ . This beam passes through a beam-splitter before it enters the tank. One beam is transmitted and goes through the tank and cell; this is the sample beam. The other reflected beam is used as a reference beam. Both beams go to two identical photometers.

We use this technique of sample and reference beams to measure the turbidity with higher accuracy. Turbidity is determined by the ratio of the light transmitted through the sample to the incident light upon the sample, so is given by,

$$\tau = \frac{1}{-L} \left[ \ln \left( \frac{I}{I_0} \right) \right]. \quad (3.1)$$

Therefore, we need to measure the light intensity just prior to the cell and the light intensity after it passes through the cell.

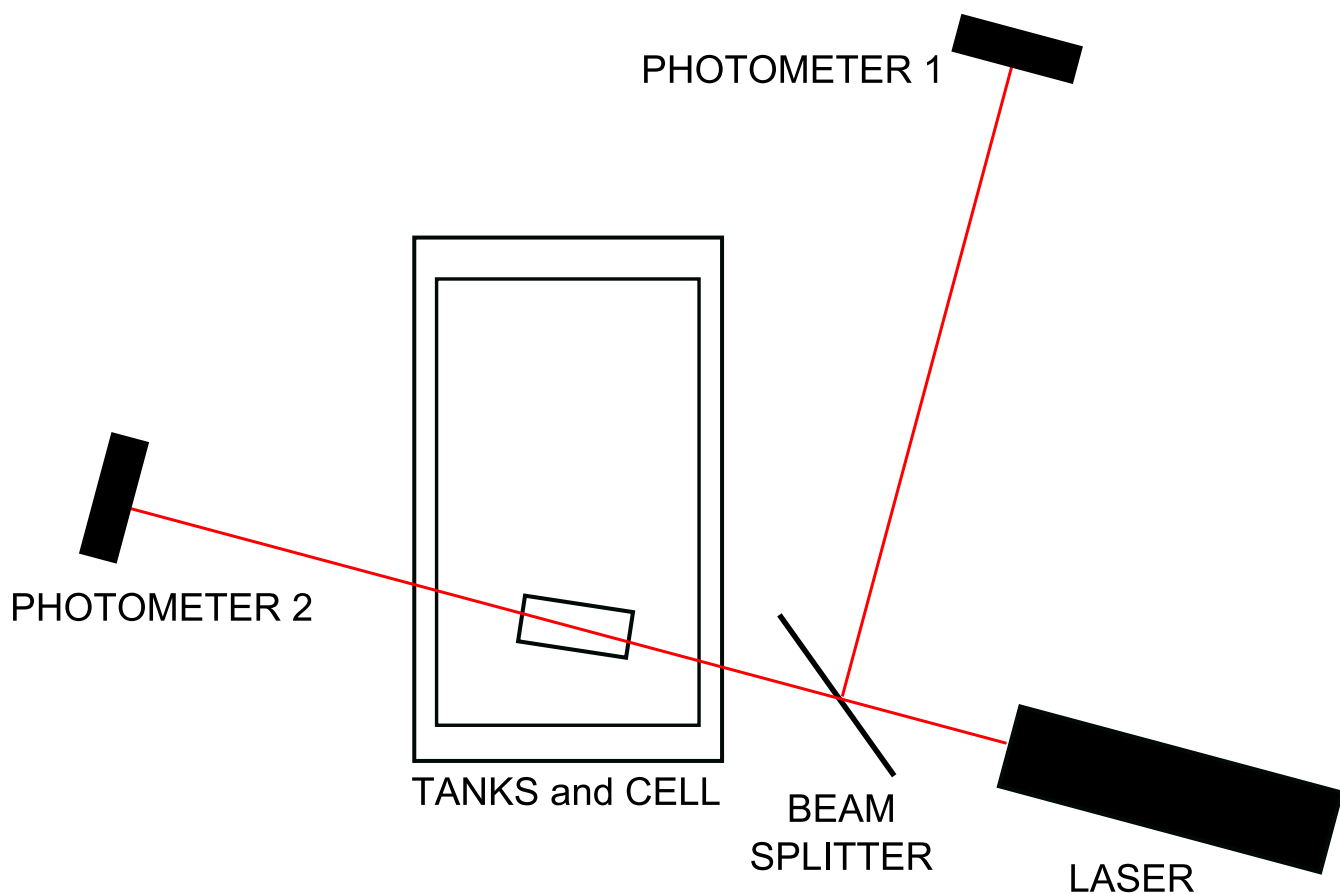


**Figure 3.3** The laser first goes through a beam splitter. The transmitted light goes through the sample and into the first photometer. The reflected light is directed toward a second photometer. This is the reference beam used to measure the incident light on the cell. The laser is pointed at an angle through the tank so that it minimizes reflections going back into the both photometers.

The intensity of the incident light from the laser is  $I_0$ . Let us call  $r$  and  $t$  the reflection and transmission emission coefficients for the light intensity after the beam splitter (with  $r + t = 1$ ). The intensity of the reflected beam from the beam splitter is  $rI_0$  and the intensity of the transmitted beam after the beam splitter is  $tI_0$ . The intensity of the light on the sample is  $tI_0$  needed in Eq. 3.1. However, we cannot measure this light intensity because it would block the light from traveling through the cell! To solve this, we measure the light intensity of the reflected beam using the logic provided below. Eq. 3.1 becomes,

$$\tau = -L^{-1} \left[ \ln \left( \frac{I_{cell}}{tI_0} \right) \right], \quad (3.2)$$

where  $I_{cell}$  is the light measured after it passes through the cell. Using the rules of logarithms we can bring out the coefficient  $t$  and add  $\ln(r) - \ln(r)$  (which is zero) to get,

$$\tau = -L^{-1} \left[ \ln \left( \frac{I_{cell}}{I_0} \right) - \ln(t) + \ln(r) - \ln(r) \right]. \quad (3.3)$$

We can bring  $-\ln(r)$  into the first natural log term,

$$\tau = -L^{-1} \left[ \ln \left( \frac{I_{cell}}{rI_0} \right) - \ln(t) + \ln(r) \right]. \quad (3.4)$$

and combine  $-\ln(t) + \ln(r)$  to get,

$$\tau = -L^{-1} \left[ \ln \left( \frac{I_{cell}}{rI_0} \right) + \ln \left( \frac{r}{t} \right) \right]. \quad (3.5)$$

Our beam splitter is a 50/50 splitter which splits the beam into two equal intensities,

$r = t = \frac{1}{2}$ , and  $\ln\left(\frac{r}{t}\right) = 0$ . Therefore Equation 3.5 becomes,

$$\tau = -L^{-1} \left[ \ln \left( \frac{I_{cell}}{rI_0} \right) \right] \quad (3.6)$$

Thus if we measure the intensity of the reflected beam,  $rI_0$ , and the intensity through the sample,  $I_{cell}$ , we can determine turbidity.

However, when we first set up the optical system we noticed that there was a significant loss of light intensity as the transmitted beam went through the tanks. We based Eq. 3.6 on the fact that when the liquid in the optical cell is completely transparent (high above  $T_c$ ),  $I = I_0$  and therefore the turbidity,  $\tau = 0$ . If the two photometers are not measuring the same intensity when  $T \gg T_c$ , Eq. 3.6 cannot be used to correctly calculate turbidity. Therefore we developed a correction factor to resolve this problem of lost light intensity through the tanks.

A new diagram can be seen in Fig. 3.4. The light that leaves the laser,  $I_L$ , is split evenly into two rays:  $tI_L$  the transmitted ray and  $rI_L$ , the reflected ray. The light going into the cell is  $tI_L$ , minus the intensity losses due to the tanks and oil,  $\Delta I_1$ . According to this,  $I_{in} = tI_L - \Delta I_1$ . What we want to measure is the intensity coming out of the cell. However, before we get to measure it, there are more losses due to the tanks and oil,  $\Delta I_2$ . This results in  $I_m$ , our measured intensity at photometer 2. We see that  $I_m = I_{out} - \Delta I_2$ . Rearranging the latter we get,  $I_{out} = I_m + \Delta I_2$ . This would give us a new equation for turbidity,

$$\tau = -\frac{1}{L} \ln \left[ \left( \frac{I_m}{tI_L} \right) \cdot \left( \frac{1 + \frac{\Delta I_2}{I_m}}{1 - \frac{\Delta I_1}{tI_L}} \right) \right]. \quad (3.7)$$

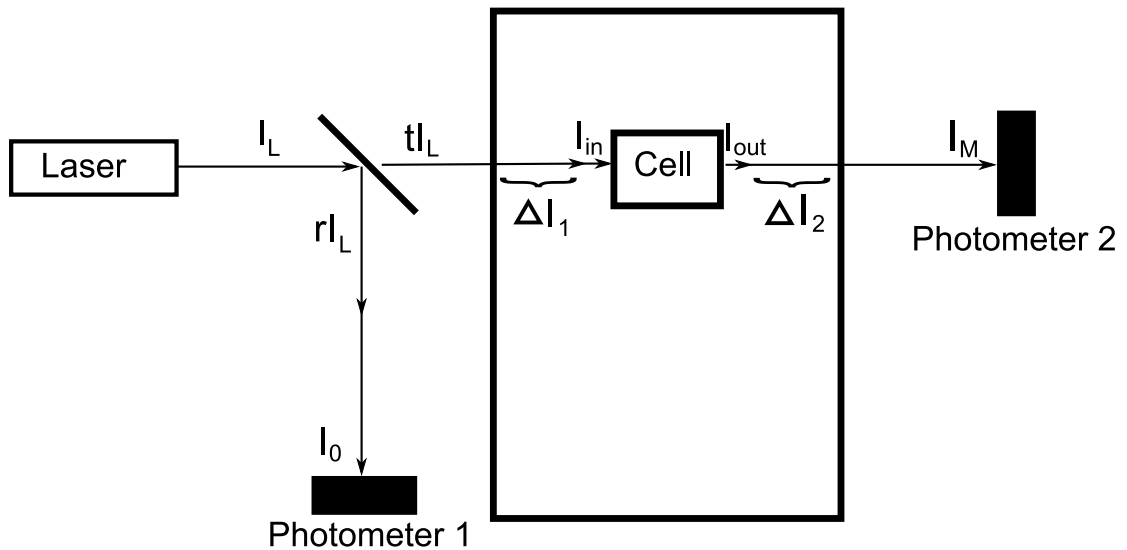


**Figure 3.4** The light that leaves the laser,  $I_L$ , is split evenly into two rays,  $tI_L$  the transmitted ray and  $rI_L$ , the reflected ray. The light going into the cell is  $tI_L$  minus the intensity losses due to the tanks and oil,  $\Delta I_1$ . What we want to measure is the intensity coming out of the cell. However, before we get to measure it there are more losses due to the tanks and oil,  $\Delta I_2$  that results in  $I_m$  our measured intensity at photometer 2. Therefore, we figured out how to approximate these losses ( $\Delta I_1$  and  $\Delta I_2$ ) to correct our intensity measurements.

Substituting in  $I_0$  for  $tI_L$  we get,

$$\tau = -\frac{1}{L} \left[ \ln \left( \frac{I_m}{I_0} \right) \cdot \left( \frac{1 + \frac{\Delta I_2}{I_m}}{1 - \frac{\Delta I_1}{I_0}} \right) \right]. \quad (3.8)$$

$\frac{\Delta I_1}{I_0}$  is the ratio of loss to input, meaning the percentage into the cell that is lost before the cell.  $\frac{\Delta I_2}{I_m}$  is the ratio of loss to output, meaning the percentage of output that is lost after the cell before exiting the fish tanks. As a first approximation let us assume that these ratios stay constant. This means that we are assuming that as the intensity of the laser light decreases the ratio of the losses to the input will decrease at the same rate. We are also assuming this is true for the ratio of loss to the output.

Therefore we can say that far above  $T_c$  where the turbidity,  $\tau = 0$ ,

$$\tau = -\frac{1}{L} \ln \left[ \left( \frac{I_m}{I_0} \right) \cdot \left( \frac{1 + \frac{\Delta I_2}{I_m}}{1 - \frac{\Delta I_1}{I_0}} \right) \right] = 0. \quad (3.9)$$

This allows us to make the conclusion,

$$-\ln \left( \frac{I_m}{I_0} \right) = +\ln \left( \frac{1 + \frac{\Delta I_2}{I_m}}{1 - \frac{\Delta I_1}{I_0}} \right). \quad (3.10)$$

So if we measure  $I_m$  and  $I_0$  far above  $T_c$  we can give them new labels,  $I_m^+$  and  $I_0^+$  and we know that the ratio of  $I_0^+$  to  $I_m^+$  will equal  $\left( \frac{1 + \frac{\Delta I_2}{I_m}}{1 - \frac{\Delta I_1}{I_0}} \right)$ . Knowing this our equation for turbidity becomes

$$\tau = -\frac{1}{L} \left[ \ln \left( \frac{I_m}{I_0} \right) - \ln \left( \frac{I_m^+}{I_0^+} \right) \right] = -\frac{1}{L} \left[ \ln \left( \frac{I_m I_0^+}{I_0 I_m^+} \right) \right]. \quad (3.11)$$

To fix the error in turbidity due to intensity losses because of the tanks we just multiply the ration of intensities  $\left( \frac{I_m}{I_0} \right)$  by a correction ratio,  $\left( \frac{I_0^+}{I_m^+} \right)$ . We measured the intensities at a temperature high above  $T_c$  and got a correction ratio of about

$\frac{I_0^+}{I_m^+} = \frac{6.5}{4.5}$ . This was added into our calculations.

## 3.4 Procedure

### 3.4.1 Determining the Critical Temperature

In order to find turbidity and therefore  $\gamma$ , the critical temperature of the cell must be calculated. The critical temperature is the highest temperature at which the two phases are indistinguishable [9]. So in some experiments the critical temperature was determined to be just before the presence of a meniscus between the two phases [9].

There are several other procedures that were used to measure this value. In one experiment, the temperature surrounding the cell was set just above the expected critical temperature and the turbidity was monitored. The critical temperature was determined when the turbidity began a more rapid, linear increase as a function of time. [17]. Another procedure noticed different transmitted intensities between the upper and bottom halves of the cell prior to a meniscus. Therefore they inferred that a phase change was happening [19].

For our experiment we decided that if the critical temperature is the highest temperature at which the two phases are indistinguishable than the appearance of a meniscus would indicate a temperature very slightly below  $T_c$ . Our sample, unfortunately was not a equal 50-50 mixture of methanol and cyclohexane. The percentage of cyclohexane in the mixture was approximately 35%. Therefore when the two liquids were in the two-phase state below  $T_c$  there was not a clear meniscus but “bubbles” of cyclohexane that would form in the methanol. Thus if we were looking for a meniscus to determine  $T_c$ , we would not be looking for a straight line across the middle of the cell, we would be looking for the formation of “bubbles.” We analyzed video of the cell undergoing the phase transitions and I found that bubbles would form at approx-

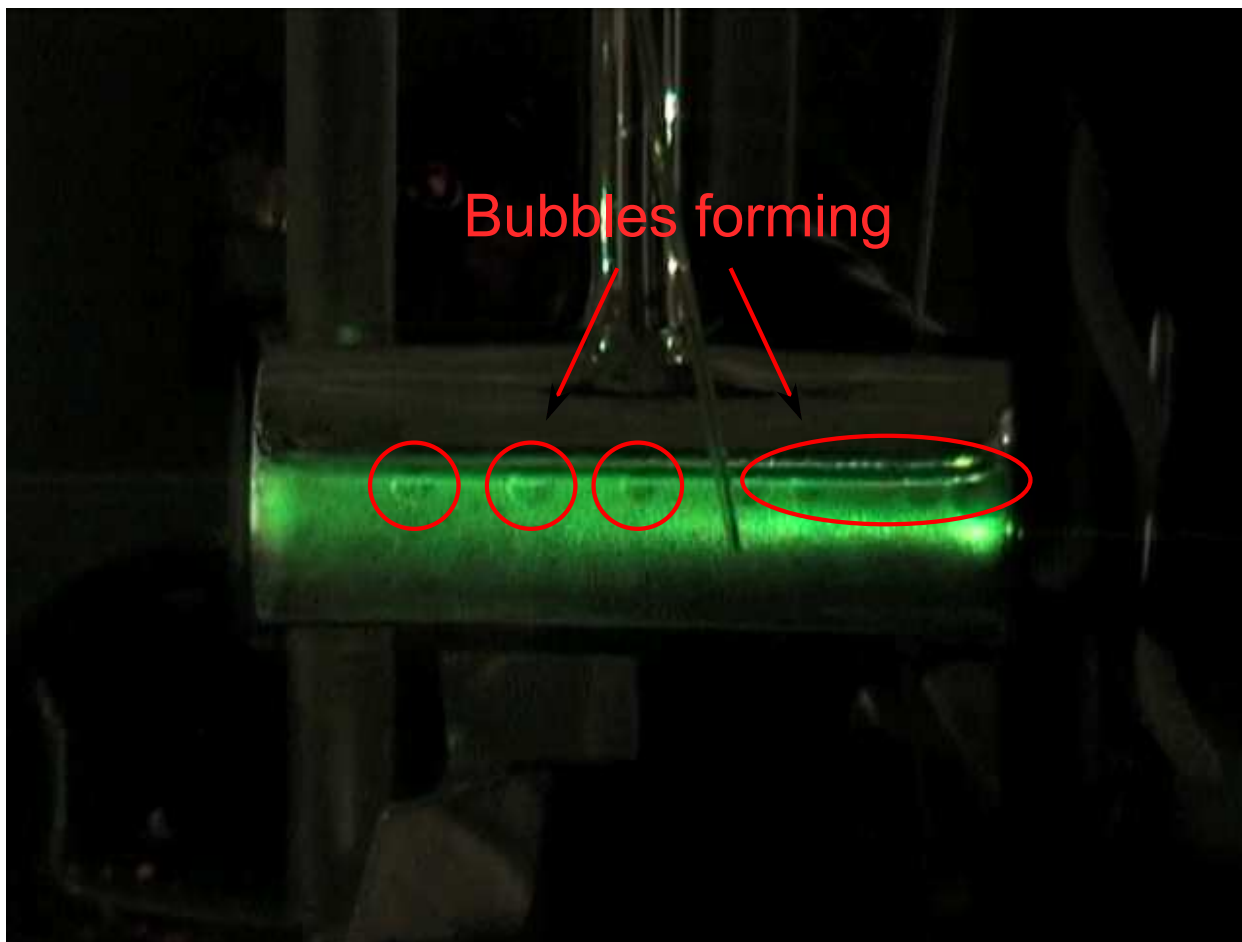


**Figure 3.5** “Bubbles” of cyclohexane start to form at  $45.8^{\circ}\text{C}$ , indicating the separation from the one phase state to the two phase state. From this we determined  $T_c = 45.8^{\circ}\text{C}$ .

imately  $45.8^{\circ}\text{C}$ . We therefore concluded that this was approximately  $T_c$ . A frame of the video can be seen in Fig. 3.5.

### 3.4.2 Light Intensity Measurement

Before any measurements can be made the cell is heated above  $T_c$ , to approximately  $50^{\circ}\text{C}$ . While the tank and cell are heated, the stirrer is on, making sure that the temperature is uniform throughout. Once the temperature has been stable at  $50^{\circ}\text{C}$  the cooling process begins.

---

For our first attempt, we shut off the stirrer and shut off the light bulbs. This created a gradient within the tank and cooled the sample down too fast to take accurate intensity measurements.

For our second attempt, we left the stirrer on after shutting off the light bulbs. This decreased the gradient, however the samples still cooled down quite rapidly.

Then we tried to leave the light bulbs on at a low power output. Without the stirrer the temperature gradient across the tank was very large. Therefore we decided that the best method would be to have the power of the light bulbs on at 25% while the stirrer was on as well, to keep the temperature gradient across the tank minimal. Flaws in this configuration will be discussed in Sec. 4.

The two beams are measured by the photometers throughout this process. The outputs of these photometers along with the thermometers are fed to the computer and the data is acquired through a LabView program. This program exports the data to a text file where it can be copied and analyzed.



# Chapter 4

## Data and Analysis

### 4.1 Turbidity

#### 4.1.1 Cool-down Trials

Before attempting to measure light intensity to determine  $\gamma$ , we must establish the optimal way to cooldown the tank. We had two variables we could vary: the light bulbs on/off and stirring on/off. From these cooldown trials, the scenario that seemed to cooldown the tank the slowest was to keep the light bulbs on at 25% power. Also to ensure that the temperature difference across the tank was minimal, the stirrer was kept on.

The first two trials of light intensity measurements showed flaws in this setup. With the light bulbs on at 25% power and the stirrer also on, small temperature fluctuations occurred due to the stirring. This resulted in unreliable intensity data. The graph of this flawed trial can be seen in Fig. 4.1. Therefore, we decided to do four test trials, alternating the use of the two variables (light bulbs on/off, and stirring on/off). Then we examined which was the optimal scenario for collecting data. The setups and their corresponding trials can be seen in Table 4.1.

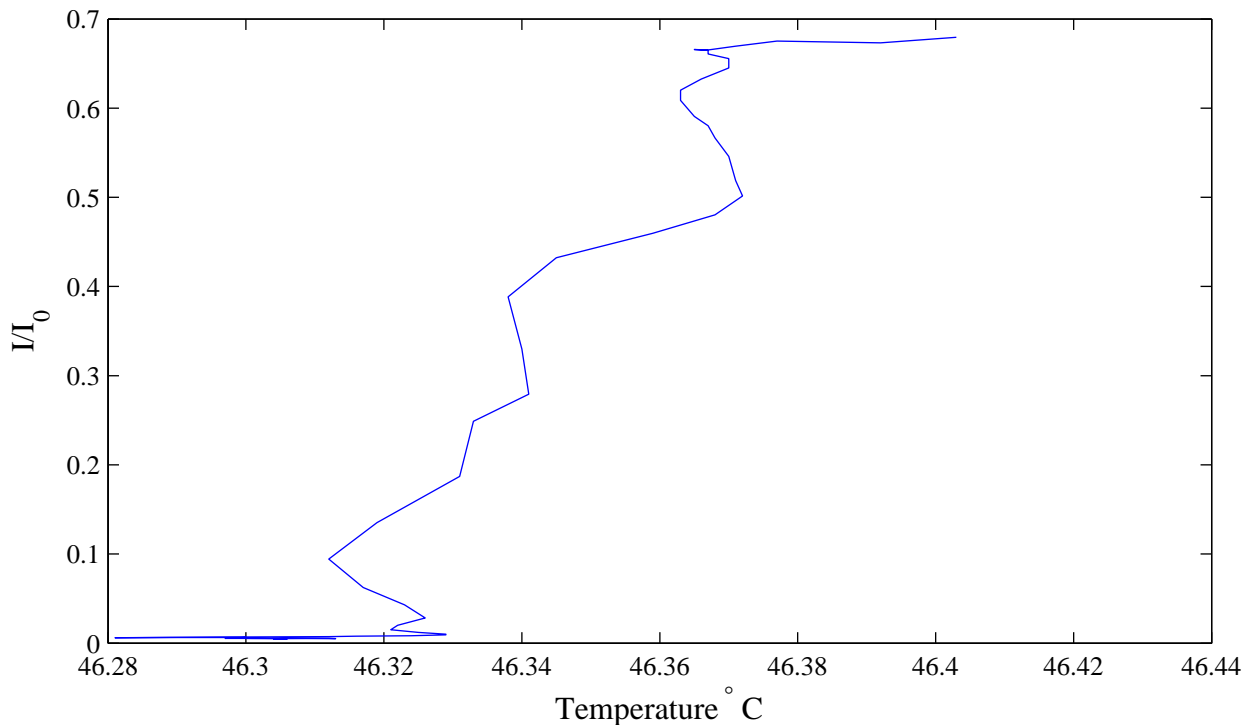


**Figure 4.1**  $I/I_0$  vs. temperature. With the light bulbs on at 25% power and the stirrer on. The stirrer clearly creates small ( $\lesssim 0.1^\circ\text{C}$ ) temperature fluctuations. Instead of a smooth curve, the intensity vs. temperature graph is an erratic line. We determined we cannot have the stirrer on.

Stirring	Light Bulb Power	Trials
ON	ON 25%	1,2
ON	OFF	3,7,8,9
OFF	ON 25%	4
OFF	OFF	5

**Table 4.1** This table shows the conditions for each trial. We decided that the light bulbs on and the stirring off were the best conditions. Therefore, we repeated them in trials 7, 8 and 9.

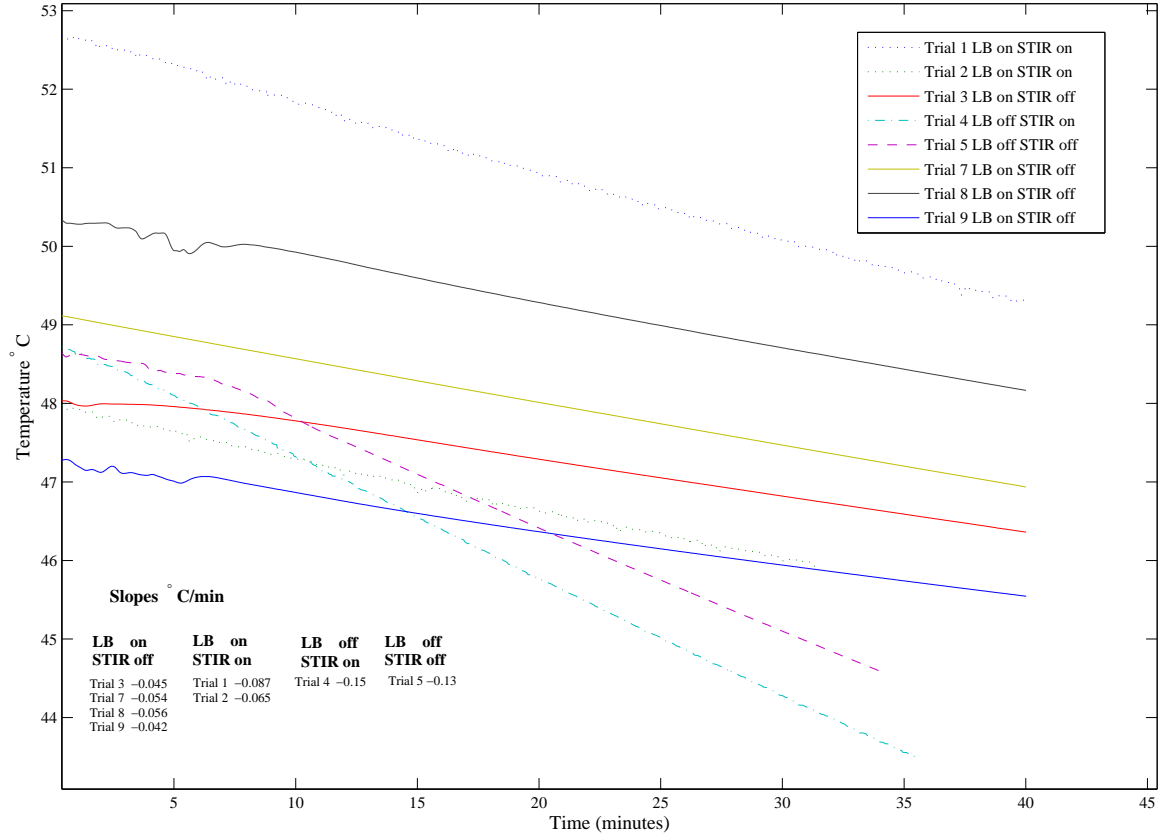


**Figure 4.2** Examination of the cool-down rates of all the trials used to determine  $\gamma$ . Trial 1 and 2 (short dashed lines) had the light bulbs on at 25% and the stirrer on. Fluctuations can be seen in both of these lines. Trials 3, 7, 8, and 9 (solid lines) were taken with the light bulbs on at 25% and the stirrer off. Trial 4 (dashed-dotted line) had the light bulbs off and the stirrer on. Trial 5 (dashed line) had both the light bulbs and the stirrer off.

The cool-down data can be seen in Fig. 4.2. The slopes of each of these trials were calculated and it was clear that the slowest rate of cool-down occurred with the light bulbs on and the stirring off. With this setup we also eliminated the temperature fluctuations. Therefore, we repeated those conditions in trials 7, 8 and 9.

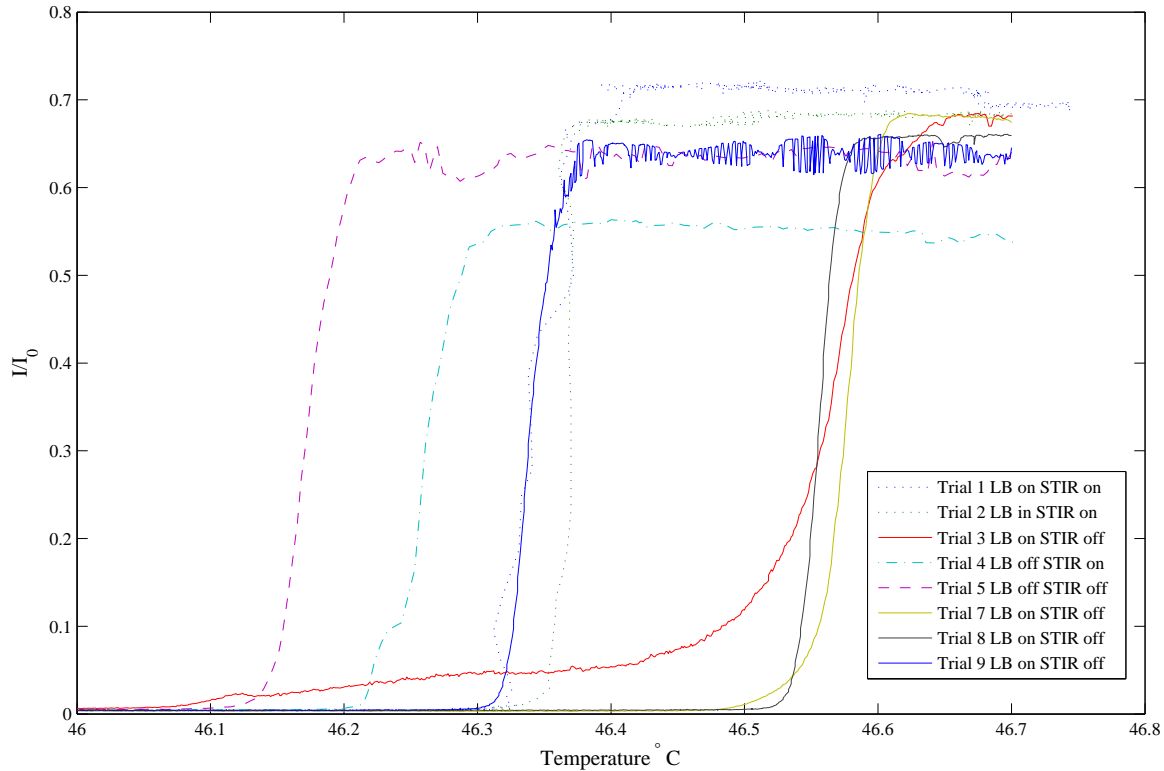


**Figure 4.3** In this graph we plotted the ratio of the measured intensity to the incident intensity vs the temperature for each trial. The erratic behavior of trials 1 and 2 show that temperature fluctuations occurred. Trials 5, 7, 8, and 9 have the same curved pattern where they drop from maximum intensity to minimum intensity with one smooth straight line.

### 4.1.2 Measuring Turbidity

For each trial we plotted the ratio of the measured intensity to incident intensity,  $\frac{I}{I_0}$  vs. the temperature,  $T$ . The results can be seen in Fig. 4.5. The curves appear to be very different however, a majority of them follow the same pattern. Trials 7, 8, and 9 follow the same smooth curve and fall from maximum intensity to minimum intensity in less than  $0.1^{\circ}\text{C}$ . Trial 3 deviates from the other three taken under the same conditions. The intensity drops suddenly similar to the other trials, however the decline to minimum intensity becomes much more gradual, overall taking approximately  $0.65^{\circ}\text{C}$ . Trial 5 (light bulbs and stirring was off), has a similar curve to 7, 8 and 9 and trial

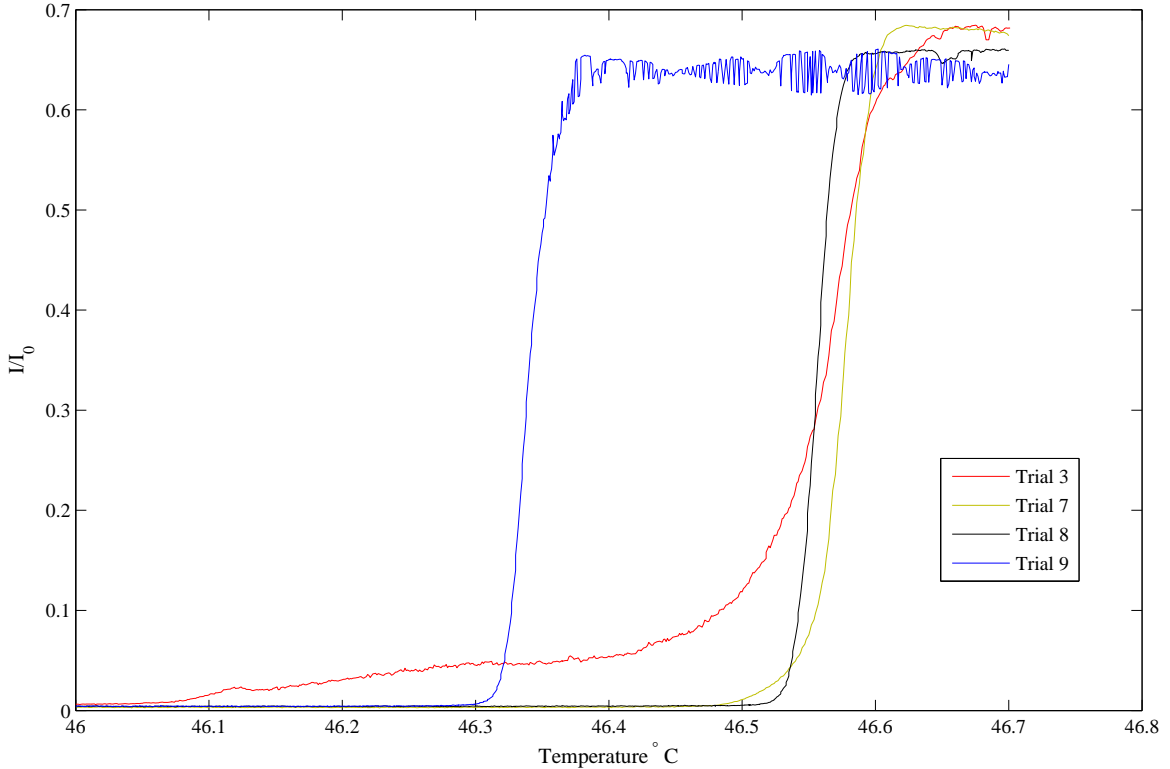


**Figure 4.4** This is a temperature vs. intensity graph for all the trials that had the light bulbs on and stirring off. Trials 7, 8, and 9 follow the same smooth curve and fall from maximum intensity to minimum intensity in less than  $0.1^{\circ}\text{C}$ . Trial 3 deviates from the other three taken under the same conditions.

4 (light bulbs on and stirring off), is also similar but has an unexplained deviated bump at the end.

Trials 3, 7, 8, and 9 were all done under the optimal conditions: light bulbs on at 25% power and the stirring off. They can be seen in Fig. 4.4. The gradual decline of trial 3 is in contrast with the abrupt decline that is represented in trials 7, 8 and 9. However, the temperature at which the intensity starts to decline is similar for trials 3, 7 and 8, approximately  $46.6^{\circ}\text{C}$ , and this temperature for trial 9 deviates by approximately  $0.2^{\circ}\text{C}$ .

### 4.1.3 Critical Exponent $\gamma$

Remember from Sec. 2.4.2 that far from  $T_c$ ,  $\tau = \frac{8}{3}\tau_0 t^{-\gamma}$  and thus,  $\log(\tau) = \log C\tau_0 - \gamma \log(t)$ . Therefore, to find  $\gamma$ , we plotted the log of the turbidity vs. the log of the reduced temperature and calculated the slope. That can be seen for all trials in Fig. 4.5. We expected to see a flat middle region like in Fig. 2.5. This is the slope

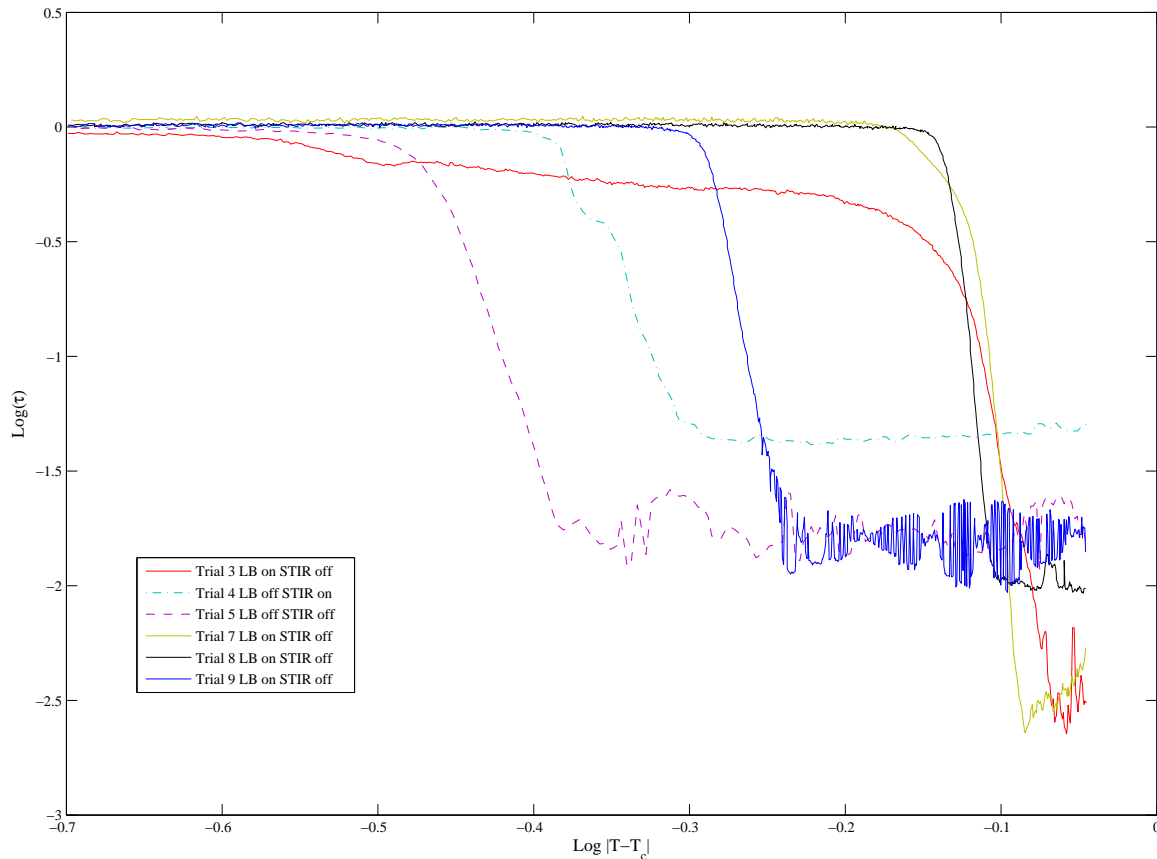


**Figure 4.5** In order to find  $\gamma$  the slope of the log-log graph of turbidity vs the reduced temperature is used. We expected to see a flat “middle” region like in Fig. 2.5 where we would calculate the slope for  $\gamma$ . However, there doesn’t seem to be a region like that on any of the trials.

that is calculated in order to find a value for  $\gamma$ . However, the shape of the graphs that we got for our data are very different from the example graph we are supposed to see. There seems to be no middle region at all. Therefore, we estimated that the sloped region is the “middle” region and we calculated the slopes for that portion of

the trials.

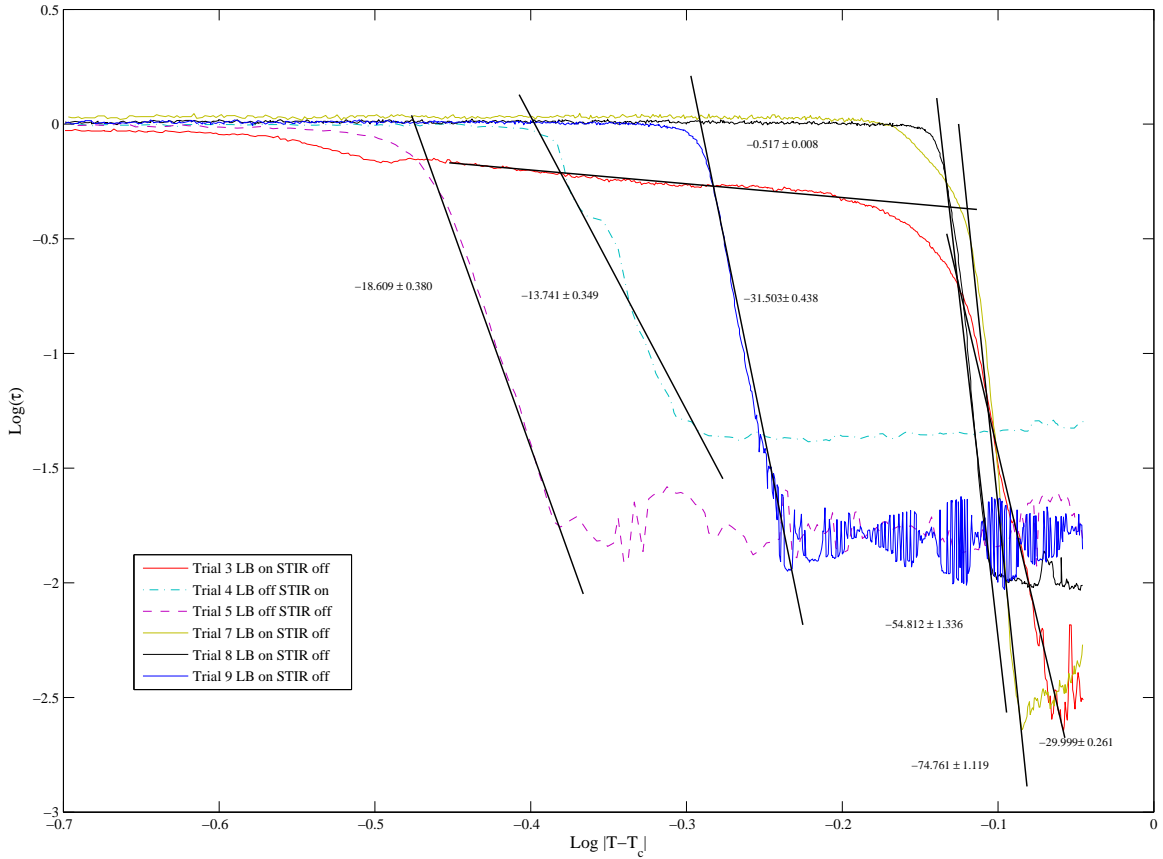


**Figure 4.6** In order to find  $\gamma$  the slope of the log-log graph of turbidity vs the reduced temperature is used. We would want to look at the slope that pertains to temperatures “far” away from  $T_c$  (on the order of  $10^{-2}$ ). We expected to see a slope of about 1.25 [20], but because there was no “middle” region as seen in Fig. 2.5, no such slope can be seen in our trials.

The temperature gets closer to  $T_c$  when you look at the graph from right to left. On the far right side of the graph, each trial has no turbidity. Alternatively on the left side of the graph, each trial has the greatest turbidity. As the trials approach  $T_c$  their turbidity increases. We are interested in the slope of this increase in turbidity because from Eq. 2.22 we know that the slope of this graph gives us the critical exponent  $\gamma$ . From predictions [20], we expect a value of 1.25, however we did not find any such slope. The middle region “far” from  $T_c$  that we showed in Fig. 2.5 is not represented

Trial	$(\gamma)$	error
3a	0.517	0.008
3b	30.0	0.3
4	13.74	0.35
5	18.6	0.4
7	75	1
8	55	1
9	31.5	0.4

**Table 4.2** In the table the possible values for  $\gamma$  are shown. These values vary greatly and are very far away from the accepted value of 1.25 [20]. There was a part of the trial 3 log graph that looked like the “middle” region we were looking for. The slope for this region was also calculated and is labeled 3a. It is closer to the predicted value but still has significant discrepancy. The larger slope for trial 3 is labeled 3b.

in our trials. Most trials show an abrupt increase in turbidity, indicated by a straight line with a negative slope. This means that the fluctuations happened very quickly, not allowing for a middle region to exist. Still, we used this region to calculate  $\gamma$  using Eq. 2.15. We calculated the slope and their errors using least squares fitting for this region. These values can be seen in Fig. 4.6 next to the black lines representing the slopes. The values calculated for  $\gamma$  and its error can be seen in Table 4.2. As seen, Fig. 4.6 and the values calculated for  $\gamma$  were not what was predicted from this experiment.

At first glance, it appears that trial 3 might have shown this slope because it exhibited a “middle” region as expected. Therefore we calculated this slope and labeled it 3a. This slope is not the same as the accepted value of 1.25, but it is a lot closer than the other trials. However, we repeated trial 3’s conditions in three additional trials and could not reproduce the same results, making trial 3 an outlier.

In Fig. 4.7 we isolated trial 8. We could have isolated 7, 8 or 9 because of the similarities in their curves, but simply chose just one trial for clarity. In this graph we show you what a slope of 1.2 would look like. However, there is no significant

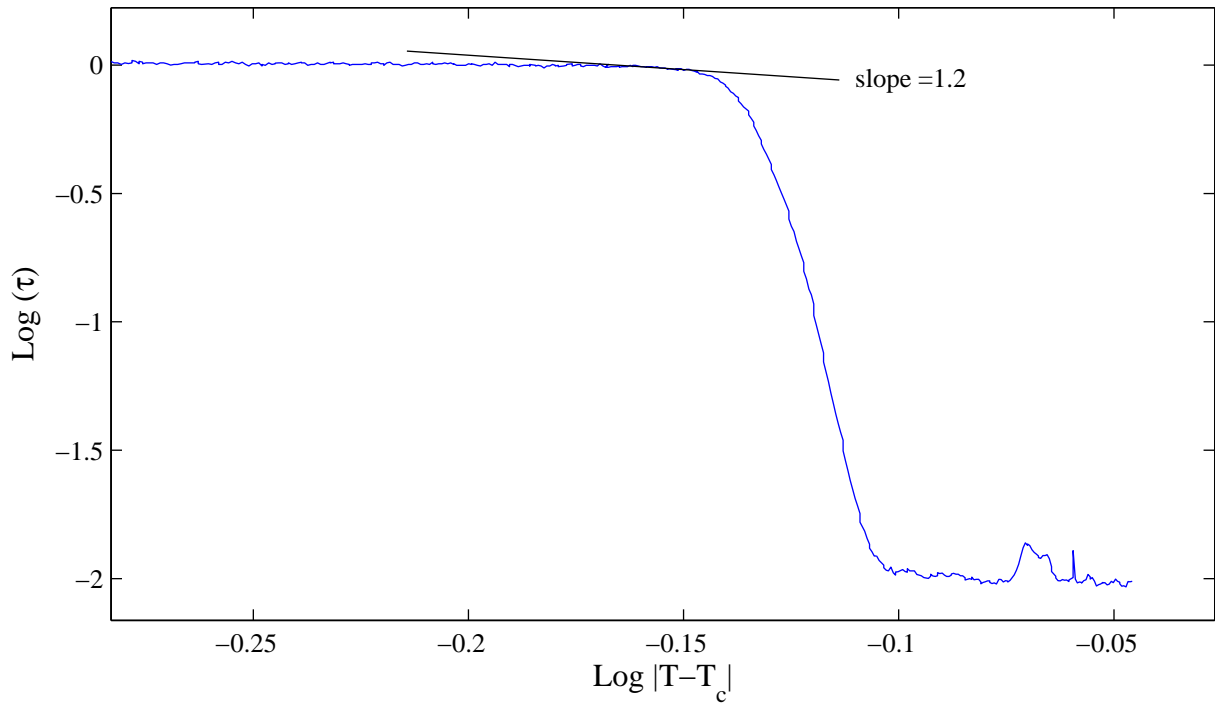


**Figure 4.7** This is only the graph of trial 8. A slope of 1.2 is shown. No significant portion of our data matches this slope.

portion of our data in this trial that matches a slope of 1.2, which exemplifies how different our data is from what was expected. The slope on the curve that we fit it to is essentially just the tangent line to that portion of the curve. We have no explanation to why our graphs do not show the slopes that we expected.

#### 4.1.4 Functional Dependence

In Section 2.4.2, Eq. 2.21 showed that very close to  $T_c$ ,  $\tau = BA - 2B\nu \ln \left| \frac{T-T_c}{T_c} \right|$ . Therefore the graph of the turbidity vs. the natural log of the reduced temperature would go as a straight line with a negative slope. Fig. 4.8 shows the graph of the turbidity vs. the natural log of the reduced temperature when very close to  $T_c$ . As mentioned earlier, because of the undetermined constants  $A$  and  $B$  in Eq. 2.21 we

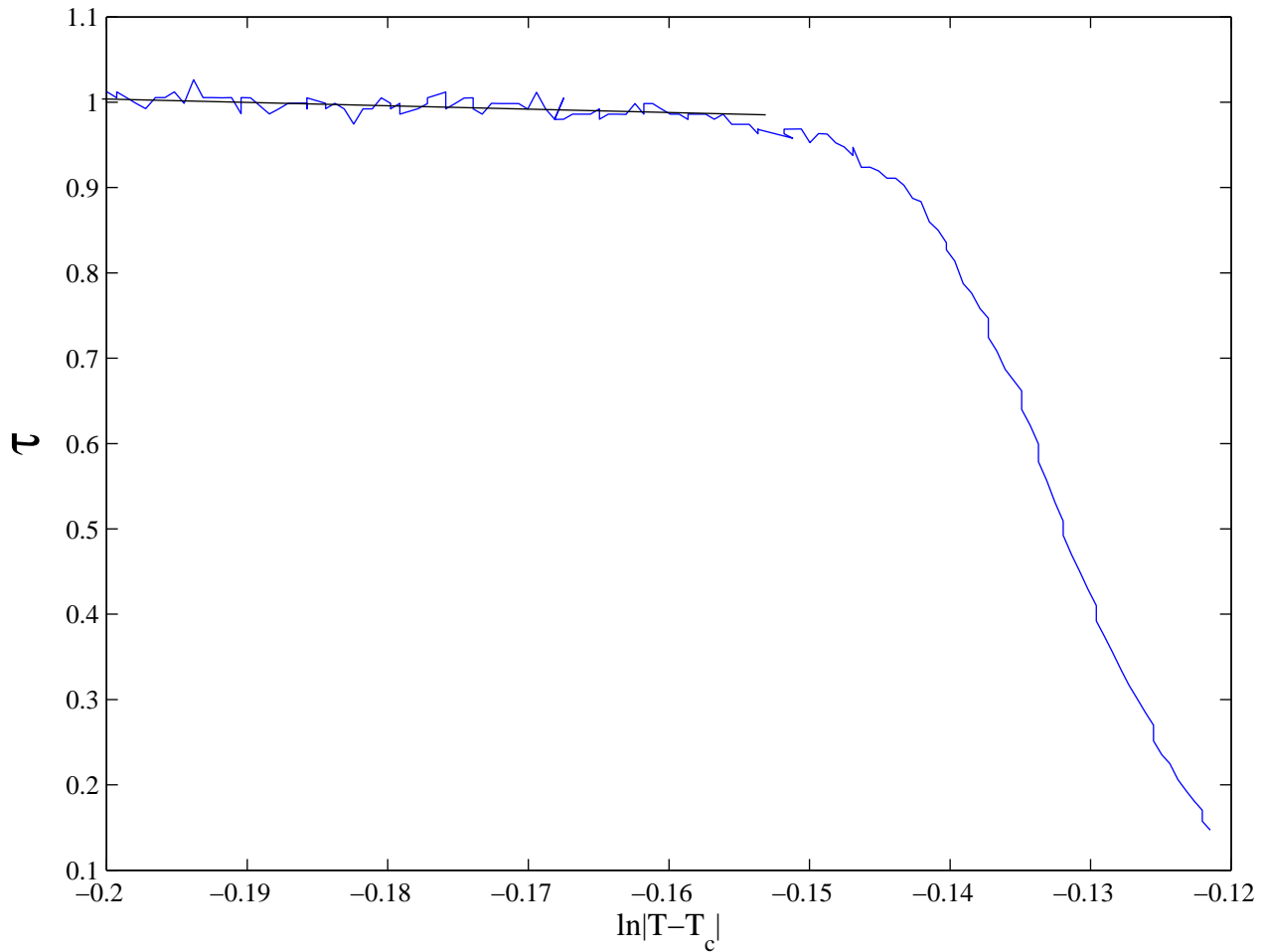


**Figure 4.8** According to Eq. 2.21 at temperatures close to  $T_c$  the graph of the turbidity vs the log of the reduced temperature should be a straight line with a negative slope. Our data imply agreement with Eq. 2.21, indicating a straight line with a negative slope.

cannot use a graph of turbidity vs. the natural log of the reduced temperature to determine  $\gamma$ . Even though the line is very noisy there is still a straight line indicating that some of our results may be valid.

# Chapter 5

## Conclusion

The exact reason why the trials did not work is unknown, however we can speculate two main reasons: chemical composition in the cell and temperature gradients in the tank. The problem with the chemical composition was that there was more methanol than cyclohexane loaded into the cell. The percentage of cyclohexane was approximately 35%. This is not concurrent with the 50-50 ratio suggested, considering the critical composition by volume for a methanol cyclohexane mixture is approximately 51.65% methanol [21]. We do not know if there was a mistake in measuring out the liquids from the beginning or if some was lost during the sealing process. This could affect a variety of factors in the experiment.

The critical temperature changes as a function of the composition of methanol in the mixture. [13] A slight difference from 50-50 would not affect  $T_c$  drastically however, our sample was not close to a 50-50 mixture. The critical temperature is essential to the calculations of the critical exponent  $\gamma$ . Therefore, if  $T_c$  is significantly different than what has been typically measured, errors in calculations can be made. Also, we defined the critical temperature as the temperature just before a meniscus is present when cooling down the sample. Cyclohexane is less dense than methanol

and so the cyclohexane formed large “bubbles” that floated in the methanol instead of making two even layers of fluid. Therefore, we did not have a meniscus per se, but instead had bubbles. To compensate, we approximated  $T_c$  to be when we started to see the formation of these small bubbles in lieu of a clear meniscus. This approach may or may not have been a valid substitution.

Finally, in regards to the cell, we could also have had water contamination. One of the most likely explanations for deviations in the critical temperature is the presence of water as an impurity in methanol. [23] We do not have the capabilities to fill and seal the cell in a dry box (a chamber filled with nitrogen gas), so the only way to suppress water contamination was to make sure the liquids were as pure as possible before loading them into the cell. This precaution was taken, however moisture in the air still could have gotten into the cell, slightly affecting the critical temperature.

The other main problem was the temperature variations in the tank. As seen from our data, the phase transition happened way too rapidly, not allowing a “middle” region in which to calculate  $\gamma$  correctly. We could not stir the mixture while taking data because of the temperature fluctuations that the stirrer creates. Therefore, there was a temperature gradient across the tank, and a temperature gradient from the bottom to the top of the tank. We realized after video analysis of various trials that the temperature gradient from the bottom to the top of the tank was significantly more detrimental to the intensity measurements. Instead of the cell becoming uniformly more opaque, the cell would start to become opaque at the bottom of the cell then slowly rise to the top. Therefore the unusual way the optical cell became opaque determined two important things: one, it determined what temperature the intensity started to decline, varying the reduced temperature for each trial, and two, it determined *the rate at which the intensity declined*. This is precisely what we used to determine the critical exponent  $\gamma$ .

The temperature at which the intensity started to decline was affected because it depended on laser position as well as temperature. As time increases the temperature of the system decreases. If the laser is shone through the bottom of the cell, the intensity will drop sooner, meaning the temperature recorded by the stationary thermometer at that time is higher than expected. If the laser is positioned to go through towards the top of the cell, by the time the solution turns opaque there, the thermometer temperature has decreased a lot more, making the recorded temperature a lot lower than expected.

The fact that the cell became opaque at the bottom of the cell and then made its way towards the top also determined the rate at which the intensity declined. If the solution had turned opaque uniformly then the intensity of light that was transmitted through the cell would have had a more gradual drop to zero. However, when the solution became opaque at the bottom of the cell it was not slightly opaque where the laser light could still transmit through. Therefore as the turbid liquid started to work its way up the cell, when it hit the laser light, the intensity would almost immediately go to zero, not allowing a gradual decline. Therefore, our calculations of  $\gamma$  were based on extrinsic factors outside of the intrinsic physical parameters that should govern the system.

## 5.1 Future Work

It is easy to see what needs to be improved in this project from the issues stated above. We need to make more cells with a better 50-50 ratio of methanol to cyclohexane. We will try the first sealing process again, that originally resulted in a broken cell, because it would prevent any fluids from possibly evaporating. Changing the composition will hopefully eliminate the varying critical temperature and the presence of “bubbles”

instead of a clear meniscus between two layers. Also, better temperature stability throughout the tank is crucial. To improve this some new ideas will be implemented. First, putting light bulbs on both sides of the tank could help in temperature gradients across the tank. Also, putting a stirrer in the tank that rotated in the x-z plane instead of on the x-y plane could facilitate mixing of the mineral oil both across the cell, and from top to bottom.

# Bibliography

- [1] J. Rowlinson, “The work of Thomas Andrews and James Thomson on the liquefaction of gases,” *Notes and Records of the Royal Society of London*, vol. 57, no. 2, p. 143, 2003.
- [2] M. Gitterman and V. Halpern, *Phase Transitions: A Brief Account with Modern Applications*. World Scientific Pub Co Inc, 2004.
- [3] R. Baierlein and G. Cook, *Thermal Physics*. 1999.
- [4] H. Stanley, *Introduction to Phase Transitions and Critical Phenomena*. 1971.
- [5] D. Goodstein, *States of matter*. Dover Pubns, 2002.
- [6] A. Sengers, R. Hocken, and J. Sengers, “Critical-point universality and fluids,” *Physics Today*, vol. 30, p. 42, 1977.
- [7] M. C. Sullivan, *The Normal-Superconducting phase transition of YBCO in zero magnetic field*. PhD thesis, University of Maryland at College Park, 2004.
- [8] R. Tolman, *The Principles of Statistical Mechanics*. Dover Pubns, 1979.
- [9] A. Mowery and D. Jacobs, “Undergraduate experiment in critical phenomena: Light scattering in a binary fluid mixture,” *Am. J. Phys*, vol. 51, pp. 542–545, 1983.

- [10] N. Wilding, F. Schmid, and P. Nielaba, "Liquid-vapor phase behavior of a symmetrical binary fluid mixture," *Physical Review E*, vol. 58, no. 2, pp. 2201–2212, 1998.
- [11] M. Fisher, "Correlation functions and the critical region of simple fluids," *Journal of Mathematical Physics*, vol. 5, p. 944, 1964.
- [12] C. Stenland and B. Pettitt, "Binary-solution critical opalescence: mole fraction versus temperature phase diagram," *Journal of Chemical Education*, vol. 72, no. 6, p. 560, 1995.
- [13] H. Marhold, P. Waldner, and G. H., "The phase diagram of cyclohexane-methanol: a challenge in chemical education," *Thermochimica Acta*, vol. 321, no. 1-2, pp. 127–131, 1998.
- [14] H. Young and R. A. Freedman, *University Physics*. Pearson Education India, 2004.
- [15] Y. Sun and Y. Xia, "Shape-controlled synthesis of gold and silver nanoparticles," *Science*, vol. 298, no. 5601, p. 2176, 2002.
- [16] V. Puglielli and N. Ford Jr, "Turbidity measurements in SF<sub>6</sub> near its critical point," *Physical Review Letters*, vol. 25, no. 3, pp. 143–147, 1970.
- [17] R. Kopelman, R. Gammon, and M. Moldover, "Turbidity very near the critical point of methanol-cyclohexane mixtures," *Physical Review A*, vol. 29, no. 4, pp. 2048–2053, 1984.
- [18] D. Jacobs, "Turbidity in the binary fluid mixture methanol-cyclohexane," *Physical Review A*, vol. 33, no. 4, pp. 2605–2611, 1986.

- 
- [19] K. Zhang, M. Briggs, R. Gammon, and J. Sengers, “The susceptibility critical exponent for a nonaqueous ionic binary mixture near a consolute point,” *Journal of Chemical Physics*, vol. 97, p. 8692, 1992.
- [20] J. Le Guillou and J. Zinn-Justin, “Critical exponents from field theory,” *Physical Review B*, vol. 21, no. 9, pp. 3976–3998, 1980.
- [21] J. Huang and W. Webb, “Diffuse interface in a critical fluid mixture,” *Journal of Chemical Physics*, vol. 50, p. 3677, 1969.
- [22] D. Lide, *CRC handbook of chemistry and physics*. CRC press, 1993.
- [23] P. Alessi, M. Fermeglia, and I. Kikic, “Liquid-liquid equilibrium of cyclohexane-n-hexane-methanol mixtures: effect of water content,” *Journal of Chemical and Engineering Data*, vol. 34, no. 2, pp. 236–240, 1989.